Atmos. Chem. Phys., 15, 4297–4316, 2015
www.atmos-chem-phys.net/15/4297/2015/
doi:10.5194/acp-15-4297-2015

Atmospheric Chemistry and Physics
Open Access

Hydroxy nitrate production in the OH-initiated oxidation of alkenes

A. P. Teng[1], J. D. Crounse[1], L. Lee[2], J. M. St. Clair[1], R. C. Cohen[2,3], and P. O. Wennberg[1,4]

[1]Division of Geological and Planetary Sciences, California Institute of Technology, Pasadena, CA, USA
[2]Department of Chemistry, University of California Berkeley, Berkeley, CA, USA
[3]Department of Earth and Planetary Sciences, University of California Berkeley, Berkeley, CA, USA
[4]Division of Engineering and Applied Science, California Institute of Technology, Pasadena, CA, USA

Correspondence to: A. P. Teng (ateng@caltech.edu)

Received: 10 February 2014 – Published in Atmos. Chem. Phys. Discuss.: 13 March 2014
Revised: 13 March 2015 – Accepted: 25 March 2015 – Published: 28 April 2015

Abstract. Alkenes are oxidized rapidly in the atmosphere by addition of OH and subsequently O_2 leading to the formation of β-hydroxy peroxy radicals. These peroxy radicals react with NO to form β-hydroxy nitrates with a branching ratio α. We quantify α for C_2–C_8 alkenes at 295 K ± 3 and 993 hPa. The branching ratio can be expressed as $\alpha = (0.045 \pm 0.016) \times N - (0.11 \pm 0.05)$ where N is the number of heavy atoms (excluding the peroxy moiety), and listed errors are 2σ. These branching ratios are larger than previously reported and are similar to those for peroxy radicals formed from H abstraction from alkanes. We find the isomer distributions of β-hydroxy nitrates formed under NO-dominated peroxy radical chemistry to be different than the isomer distribution of hydroxy hydroperoxides produced under HO_2-dominated peroxy radical chemistry. Assuming unity yield for the hydroperoxides implies that the branching ratio to form β-hydroxy nitrates increases with substitution of RO_2. Deuterium substitution enhances the branching ratio to form hydroxy nitrates in both propene and isoprene by a factor of $\sim$1.5. The role of alkene chemistry in the Houston region is re-evaluated using the $RONO_2$ branching ratios reported here. Small alkenes are found to play a significant role in present-day oxidant formation more than a decade (2013) after the 2000 Texas Air Quality Study identified these compounds as major contributors to photochemical smog in Houston.

1 Introduction

The formation of alkyl nitrates is an important process controlling tropospheric oxidants and the lifetime of NO_x. During daytime, alkyl nitrates form via a radical chain terminating branch in the reaction of alkyl peroxy radicals with NO. The major branch in this chemistry recycles HO_x and produces ozone. The fate of alkyl nitrates is thought to be determined by either (1) deposition leading to loss of atmospheric NO_x or (2) further reactions that lead to recycling of NO_x or conversion of the organic nitrates to HNO_3. Thus, $RONO_2$ can serve either as a permanent sink or as a transport mechanism for NO_x.

Alkyl nitrates also play an important role in organic aerosol formation (Rollins et al., 2012; Brown et al., 2009). Aerosol nitrates have been observed to form as a result of NO_3 chemistry, though our understanding of the gas phase mechanisms leading to aerosol nitrate remains incomplete.

Knowledge of the branching ratio of $RO_2 + NO$ to form alkyl nitrates from RO_2 derived from specific volatile organic compounds (VOCs) is important for diagnosing the role of individual VOCs in ozone and aerosol formation. This knowledge can then guide specific control strategies to mitigate pollution (Ryerson et al., 2003; Rosen et al., 2004; Farmer et al., 2011).

Many previous studies have reported VOC-specific branching ratios to form alkyl nitrates. These studies suggest that the branching ratios increase with increasing carbon number, increasing pressure, and decreasing temperature (Orlando and Tyndall, 2012, and references therein). This behavior has been interpreted as evidence that the lifetime of the O–ONO intermediate controls the fraction of the nascent complex that isomerizes onto the ONO_2 surface. The dynamics that lead from the peroxynitrite (ROONO) to the nitrate ($RONO_2$) is, however, not well understood (Lohr et al., 2003; Barker et al., 2003; Zhang et al., 2002).

Alkenes react rapidly by addition of OH and O_2 to form β-hydroxy peroxy radicals. These peroxy radicals react with NO to form β-hydroxy nitrates.

Previous studies have suggested that the branching ratio to form β-hydroxy nitrates from reaction of β-hydroxy peroxy radicals with NO is lower than for peroxy radicals produced from reactions of alkanes of the same carbon number with OH (O'Brien et al., 1998). The lower nitrate branching ratios for β-hydroxy peroxy radicals have been attributed to the β-hydroxy group weakening the O–ONO bond, shortening the lifetime of the OONO complex toward decomposition to NO_2 and thereby reducing the time available to sample the crossing to the nitrate surface ($RONO_2$) (Muthmuruthma et al., 1993; O'Brien et al., 1998; Matsunga and Ziemann, 2009, 2010). Patchen et al. (2007), however, reported the branching ratio to form hydroxy nitrates derived from 1- and 2-butene as larger than previously reported by O'Brien et al. (1998). This study was conducted at 100 torr where $RONO_2$ yields should be smaller than at atmospheric pressure. Additional studies conducted on alkenes using long-path FT-IR have determined total alkyl nitrate yields similar to those determined for *n*-alkanes. However, these studies provide only upper bounds for branching ratios to $RONO_2$ due to the possible formation of organic nitrate from $RO + NO_2$ chemistry (Atkinson et al., 1985; Tuazon et al., 1998; Aschmann et al., 2010).

In this study, we use CF_3O^- CIMS (chemical ionization mass spectrometry) to quantify the hydroxy nitrates yield. In addition, we utilize gas chromatography with both CF_3O^- CIMS and thermal dissociation NO_2 laser-induced fluorescence (TD-LIF) to resolve and quantify isomeric distributions of these hydroxy nitrates. The TD-LIF instrument provides independent confirmation that the observed signals are alkyl nitrates and enables secondary calibration of CF_3O^- CIMS sensitivity by the TD-LIF for individual β-hydroxy nitrates.

2 Materials and methods

1-propene (propene) (> 99 %), d_6-propene (> 99 %), 1-butene (but-1-ene) (> 99 %), *cis*-2-butene (*cis*-but-2-ene) (> 99 %), methylpropene (2-methylpropene, isobutylene, isobutene) (> 99 %), 1-pentene (pent-1-ene) (> 98 %), 2-methyl 1-butene (2-methyl but-1-ene) (> 98 %), 2-methyl 2-butene (2-methyl but-2-ene) (> 99 %), isopropyl nitrate (nitric acid, 1-methylethyl ester) (> 99 %), 1-hexene (hex-1-ene) (> 99 %), 1-octene (oct-1-ene) (> 98 %), and 1,2-butanediol (butane 1,2 diol) (> 98 %) purity were purchased from Sigma Aldrich and used without further purification. Hydrogen peroxide (30 and 50 % by weight in water) was purchased from Sigma Aldrich. Ethene (ethylene) (> 99 %) was purchased from Scott Specialty Gases. A nitric oxide (NO) (1994 ± 20 ppmv in ultra high purity N_2) standard gas tank for chamber experiments was prepared by Matheson. Nitrogen dioxide (NO_2) (5 ppmv in ultra high purity N_2) gas tank for TD-LIF calibration was prepared by Matheson. Methylnitrite (CH_3ONO) was synthesized, purified, and stored using methods similar to those described by Taylor et al. (1980).

2.1 Environmental chamber experiments

The CIMS and thermal dissociation laser-induced fluorescence instrument (TD-LIF) instruments and the Teflon reaction chamber have been described previously (Crounse et al., 2013; Lee et al., 2014). Briefly, photochemical experiments were conducted in a 1 m^3 enclosure composed of fluorinated ethylene propylene copolymer (Teflon FEP, Dupont). UV photolysis of hydrogen peroxide (H_2O_2) or methyl nitrite (CH_3ONO) provided the primary HO_x source. Experiments to determine the hydroxy nitrate yields were typically conducted with initial mixing ratios of 0.08–2 ppmv of alkene, 0.2–2 ppmv (±10 %) of hydrogen peroxide or 40–200 ppbv methyl nitrite, and 0.5–4 ppmv (±5 %) of NO. Experiments to determine hydroxy hydroperoxide isomeric distributions were conducted with initial mixing ratios of 2–30 ppbv alkene and 2–20 ppmv of hydrogen peroxide. All experiments were performed at ambient pressure, approximately 993 hPa. Table 1 provides a complete list of experiments.

Alkene or CH_3ONO addition to the environmental chamber was accomplished by first flushing a 500 cm^3 glass bulb with the compound and then filling it to the desired pressure (1–20 hPa). The bulb was then filled with N_2 gas to 993 hPa. If required, the compound was serially diluted by pumping the bulb down to the desired pressure (5–400 hPa) and backfilling again with N_2 to atmospheric pressure. The concentrations of ethene, propene, 1-butene, 2-methyl propene, 2-methyl 2-butene, 2-methyl 1-butene, 1-hexene and 1-octene were determined within the bulb by FT-IR spectroscopy. FT-IR cross sections were obtained from the PNNL (Pacific Northwest National Laboratory) database (Johnson et al., 2002; Sharpe et al., 2004) for all compounds except *cis*-2-butene and d_6-propene. Determinations of the concentrations of d_6-propene and *cis*-2-butene were based on manometry, and checked against GC-FID (gas chromatography flame ionization detector) measurements relative to the other gases added in the same experiment assuming equivalent FID signal per carbon atom. These independent methods agreed to within 3 %.

NO addition was accomplished by evacuating a 500 cm^3 glass bulb, and filling from the standard tank to the desired pressure. NO was added to the enclosure only after at least 0.25 m^3 of air was added to lessen conversion of NO to NO_2 from the reaction of $2NO + O_2$. All pressure measurements were obtained using 13.3 or 1333.3 hPa full scale absolute pressure gauges (MKS Baratron™). H_2O_2 addition was accomplished by evaporating a known mass of 30 or 50 % by

Table 1. Experiment list.

Experiment. #	H_2O_2 ppmv	NO ppbv	VOC, ppbv			Absolute α	Relative α	ROOH yield	TD-LIF measurement
1	2	500	propene, 96	ISOPN, 50					x
2	2	500	propene, 93	ISOPN, 38					x
3	2	500	propene, 116	ISOPOOH, 38		x			
4	2	500	propene, 164	ISOPOOH, 50		x			
5		500	propene, 143	ISOPOOH, 44	CH_3ONO, 350	x			
6		500	propene, 156	ISOPOOH, 20	CH_3ONO, 370	x			
7	2.5	1200	propene, 262	1-butene, 183	1-pentene, 238	x			
8	2.5	1100	propene, 270	2-methyl 1-butene, 185	1-hexene, 180	x			
9	2.5	2300	propene, 235	1-hexene, 210		x			
10	2.5	1200	propene, 408	1-hexene, 390		x			
11	2.5	600	propene, 133	1,2 butanediol, 80		x			
12	1.0	600	propene, 162	1,2 butanediol, 490		x			
13	1.0	700	propene, 164	1,2 butanediol, 70		x			
14		600	propene, 122,	1,2 butanediol, 70	CH_3ONO, 60	x			
15	2	500	1-butene, 131	1-hexene, 105		x			x
16	2	500	1-butene, 15	*cis*-2-butene, 120		x			x
17	2	500	ethene, 1096	*cis*-2-butene, 115		x			x
18	2	500	2-methyl 2-butene, 107			x			x
19	2	500	methylpropene, 342			x			x
20	2.6		propene, 9					x	
21	2.6		propene, 8					x	
22	2.6		propene, 5					x	
23	10.4		propene, 7					x	
24	2		propene, 21					x	
25	2		propene, 36	1-butene, 17	1-hexene, 33			x	
26	2		propene, 30	butadiene, 14	2-methyl 2-butene, 20			x	
27	2.7		1-hexene, 5					x	
28	2.7		2-methyl 2-butene, 4					x	
29	2.8		methylpropene, 4					x	
30	2.8		1-butene, 7					x	
31	2	1000	d_6-propene, 324	1-butene, 256			x		
32	2	1000	d_6-propene, 280	propene, 334.5	1-butene, 102		x		
33	2	1140	ethene, 963	propene, 426	methylpropene, 261		x		
			2-methyl 2-butene, 242	1-hexene, 254	1-octene, 326				
34	0.2	1930	ethene, 2983	propene, 608	methylpropene, 309		x		
			2-methyl 2-butene, 339	1-hexene, 263	1-octene, 314				
35	0.2	950	propene, 1418	1-butene, 85	methacrolein, 902		x		
			2,3 dimethyl,2-butene, 1096						
36	0.2	950	propene, 1380	methyl vinyl ketone, 1258	*cis*-2-butene, 674		x		
			2,3-dimethyl 2-butene, 732						
37	20		methylpropene, 181					x	

weight H_2O_2 in water. Concentrations were confirmed by CIMS measurement of hydrogen peroxide in the gas phase.

The composition of the chamber was monitored by sampling from the enclosure at ~ 2000 sccm through a single 4 mm ID perfluoroalkoxy line with instruments sampling in series: (1) ToF-CIMS (Tofwerk, Caltech), (2) Triple Quadripole MS-MS CIMS (Varian, Caltech), (3) GC-FID (HP 5890 II), (4) NO_x Monitor (Teledyne 200EU), (5) O_3 Monitor (Teledyne 400E). Sampling conducted this way minimizes surface interactions by lowering the residence time of chamber air in the sampling line to < 0.2 s. The sampling configuration in which chamber air passes only through a Teflon sampling line without first entering a gas chromatograph is referred to here as "direct" sampling. The specifics of the CIMS have been described in detail elsewhere (Crounse et al., 2006, 2011, 2012, 2013; Paulot et al., 2009; St. Clair et al., 2010).

Reaction products were monitored using CF_3O^- chemical ionization mass spectrometry (CIMS) methods. Multifunctional products from alkene oxidation were detected using CF_3O^- cluster ion signals observed at m/z $M + 85$ product. The following m/z were used for hydroxy nitrate determination: ethene, 192; propene, 206; d_6-propene, 212; 1-butene/*cis*-2-butene/methylpropene, 220; 2-methyl,2-butene/1-pentene/2-methyl 1-butene, 234; 1-hexene 248; 1-octene, 276. For hydroxy hydroperoxides, the following m/z were used for quantification: propene, 177; 1-butene/methylpropene, 191; 2-methyl 2-butene, 205; 1-hexene, 219. 1,2 butanediol was monitored using signal at m/z 175, and the resulting hydroxycarbonyls were monitored m/z 173.

The alkene concentrations were monitored using an GC-FID (Agilent 5890). Chamber air was sampled into a 10 cm^3 stainless steel sample loop or a 30 cm^3 PFA (perfluoroalkoxy) sample loop using a six-port valve. The sample

was transferred to the head of the column in the oven at temperatures between 308 and 373 K, depending on the hydrocarbon. In the case of ethene, samples were cryotrapped with liquid nitrogen on the head of the column. A megabore (0.53 mm) 30 m Plot-Q column (Agilent J & W columns) was used to separate compounds using 7–9 standard $cm^3\,min^{-1}$ N_2 carrier gas. A suitable temperature ramp was selected for each compound.

2.1.1 GC-CIMS/LIF chromatography

After oxidation, the chamber air was analyzed using GC-CIMS/LIF (gas chromatography CF_3O^- CIMS/TD-LIF). Chamber air is pulled through a Teflon sampling line, through a Teflon three-port valve, and cryofocused at 240–280 K on the head of a 4 m megabore HP 612, a 4 m megabore RTX-1701, or 1 m megabore RTX-1701 column. Columns were held inside a Varian GC oven (CP-3800). Following the GC, the column effluent was split between the ToF-CIMS instrument and the TD-LIF system for the experiments listed in Table 1. For all other experiments where the TD-LIF instrument was not used, the column effluent flowed directly to the ToF-CIMS. After a measured flow of chamber air ranging from 30 to 200 standard cm^3 was cryofocused over a length of time ranging from 2 to 12 min by placing the GC column in a cooled (−20 °C) isopropanol bath, the three-port valve was switched to allow carrier gas (N_2) to flow through the GC column. The volume of chamber air cryofocused in this manner was determined by the collection time and the flow rate (inferred from manometry). Carrier gas flow was controlled by a mass flow controller (MKS) at 8.7 standard $cm^3\,min^{-1}$ N_2. Temperature program (30 °C, hold 0.1 min, 3 °C min^{-1} from 30–60 °C, 10 °C min^{-1} to 130 °C, hold 3 min) started approximately 2–3 min after cryofocusing. All wetted surfaces in the analytical setup were comprised of Teflon, PEEK, or GC column materials to limit surface interactions.

The TD-LIF system sampled a portion of the GC carrier gas into 400 °C oven. Pure O_2 is added to this flow upstream of the TD oven to ensure complete conversion of $RONO_2$ to NO_2. NO_2 is measured using laser-induced fluorescence (Lee et al., 2014). The system was calibrated at the same operating pressure with a standard tank of NO_2. The conversion efficiency of the TD-LIF was evaluated with isopropyl nitrate and found to be 100 % (see Appendix B). We assume here that conversion of other $RONO_2$ is also 100 %. To the extent the conversion of these hydroxy nitrates to NO_2 is less than 100 %, the reported branching ratios are biased low.

The ToF-CIMS instrument was operated in the same manner as during the photochemistry with diluted column effluent substituting for the ambient flow. With this split flow configuration, the concurrent elution of alkyl nitrates was monitored by both the ToF-CIMS and TD-LIF instruments, enabling secondary calibration of the CIMS sensitivity by the TD-LIF to the individual alkyl nitrates.

The determination of the split ratio (approximately 10 : 1) between the CIMS and TD-LIF NO_2 instrument was performed using an isopropyl nitrate standard (80 ppbv in air) prepared in the same fashion as the alkenes described above. The gas standard was both directly sampled from the chamber and following cryo-collecting $\sim 200\,cm^3$ on an HP 612 column and eluting the peak in the usual GC configuration. The signal level in the TD-LIF instrument was recorded as the GC ramped through its usual temperature program. Signal levels were also compared between direct measurement of $\sim$ 80 ppbv isopropyl nitrate within a Teflon bag into the TD-LIF system and collected for 4 min on a cooled sample loop. A separate check was also conducted with prepared standards of isoprene hydroxy nitrates in which the standard was directly sampled from the chamber and through the GC system. This measurement was problematic due to long equilibration times (> 3 h) resulting from low sampling flow limited by the small diameter tubing in the TD-LIF optimized for GC use. The TD-LIF was also calibrated at the end of each photochemistry experiment with gas standard of 5 ppmv NO_2 in N_2 (Matheson) under matching pressure conditions.

2.1.2 Experiments to determine hydroxy nitrate branching ratios relative to propene

Experiments 31–36 (Table 1) were conducted to determine the β-hydroxy nitrate yields from alkenes relative to the β-hydroxy nitrate yield from propene. These experiments involved simultaneous oxidation of up to six alkenes. Initial alkene concentrations were determined by FT-IR spectroscopy. The chamber was monitored for at least 20 min to determine the background signals. UV lights were turned on for a period (< 10 min) sufficient to achieve a hydroxy nitrate concentration high enough for quantification while minimizing secondary OH losses of hydroxy nitrates. Less than 10 % of each alkene species was oxidized in each experiment. Experiments were initiated between 292 and 293 K and the temperature rise was no more than 1 K over the course of the experiments. Hydroxy nitrate branching ratios were determined relative to those of propene with the exception of Experiment 31, which measured d_6-propene hydroxy nitrate branching ratios relative to 1-butene. Accurate GC-FID quantification in these experiments was not possible due to the small change in concentration of each compound.

2.1.3 Experiments to determine hydroxy nitrate branching ratios in an absolute manner

Experiments 1–19 (Table 1) were conducted to determine the absolute branching ratios to form β-hydroxy nitrates. Experiments involved addition of 1–3 alkenes, NO, and H_2O_2 or CH_3ONO into the chamber. Initial alkene concentrations were determined by FT-IR and confirmed by manometry and GC-FID peak areas. Isoprene hydroxy nitrates or isoprene hydroxy hydroperoxides were also added to the chamber in

Experiments 1–7 to measure their OH rate constants relative to propene as described in experiments of Lee et al. (2014) and St. Clair et al. (2015). To measure OH exposure, 1,2 butane diol (a reference compound measurable by CIMS) was added to a series of experiments to confirm the alkene decay measured by GC-FID. In these experiments, UV lights were turned on until a significant and quantifiable decay of hydrocarbon was observed (> 15 %) on the GC-FID. Experiments were initiated between 292 and 293 K, and the temperature increased by at most 7 K after the lights were turned on.

2.1.4 Experiments to determine hydroxy hydroperoxide isomer distributions

Experiments 20–30 (Table 1) were conducted to determine the hydroxy hydroperoxide isomer distributions. Experiments involved addition of 1–3 alkenes and H_2O_2. Initial alkene concentrations were determined by FT-IR spectroscopy. UV lights were turned on until a measurable concentration of hydroxy hydroperoxides was produced. Less than 10 % of each alkene species was oxidized in each experiment as indicated by GC-FID signal areas.

2.1.5 Post-experiment GC-CIMS/TD-LIF monitoring

Following each experiment, products were analyzed by GC-CIMS/TD-LIF or GC-CIMS. At least three replicate GC runs were conducted. Transmission through the CIMS portion of the GC-CIMS/TD-LIF was measured by comparing the direct sampling measurement to the integrated chromatogram signal for a given m/z. The integrations were corrected by blank GC runs (less than 3 % signal in all cases over the elution time of the hydroxy nitrate peaks). The transmission was determined by the ratio of the direct sampling and the total chromatogram signals after taking into account the sampling flow-rate differences.

3 Results and discussion

The following analysis procedure was used to calculate branching ratios from the experimental data:

1. β-hydroxy nitrate CIMS sensitivities are determined from simultaneous measurement of hydroxy nitrates by cryofocused gas chromatography.
2. The fraction of the reaction of OH that proceeds via addition, f_a, is estimated from previously reported kinetic data on alkenes. This allows normalization of subsequent measurements of the yields of β-hydroxy nitrates, $Y_{\beta HN}$, to produce branching ratios, α.
3. Branching ratios to form hydroxy nitrates, α, from alkenes relative to $\alpha_{HN\_propene}$ are determined through experimental data. These results allow direct comparison of the dependence of α on structure. α is well described by a linear relationship: $\alpha = m \times N + b$, where α is isomer-averaged branching ratio, and N is the number of heavy atoms in the peroxy radical (not counting the peroxy radical oxygens).
4. The absolute branching ratios, α, are determined using absolute quantification of alkene and hydroxy nitrate concentrations. The dependence of α on the number of heavy atoms, N, is derived.
5. The entire absolute branching ratio data set is used to place all relative nitrate branching ratios on an absolute basis.
6. Isomer specific distributions for alkenes are derived using GC chromatograms of hydroxy nitrate isomers.
7. The OH addition branching ratios are inferred by analyzing hydroxy hydroperoxide isomer distributions of alkenes oxidized by OH under HO_2-dominated conditions.
8. The dependence of the alkyl nitrate branching ratios on the type (i.e., primary, secondary or tertiary) of β-hydroxy RO_2 radicals is determined by comparing (5) and (6).

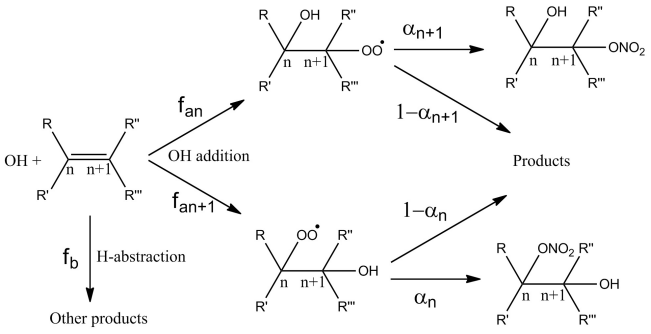

Figure 1. Reaction pathways of alkenes with OH. OH oxidation with alkenes follows two pathways: OH addition (f_n and f_{n+1}) and H-abstraction (f_{ab}, where $f_{ab} = \sum_{n=1}^{l} f_{abn}$). $f_a + f_{ab}$) = 1. Subscripts indicate the carbon number at which either OH addition or abstraction occurs. For alkenes studied in this work at room temperature, the sum of f_{an} and f_{an+1} is much greater than f_{ab}. See text for further discussion of estimations for f_{ab}.

We define the branching ratio (α_n) to represent the fraction of $RO_2 + NO$ reaction that produces $RONO_2$, where the subscript n denotes the carbon alpha to the peroxy radical (Fig. 1). We define the fraction of OH that adds to carbon n as f_{an} out of the total OH + alkene reaction. The total fraction of OH + alkene that proceeds via addition is given as $f_a = \sum_{n=1}^{l} f_{an}$. The total fraction of OH + alkene that proceeds via H-abstraction is given as $f_{ab} = \sum_{n=1}^{l} f_{abn}$, where the

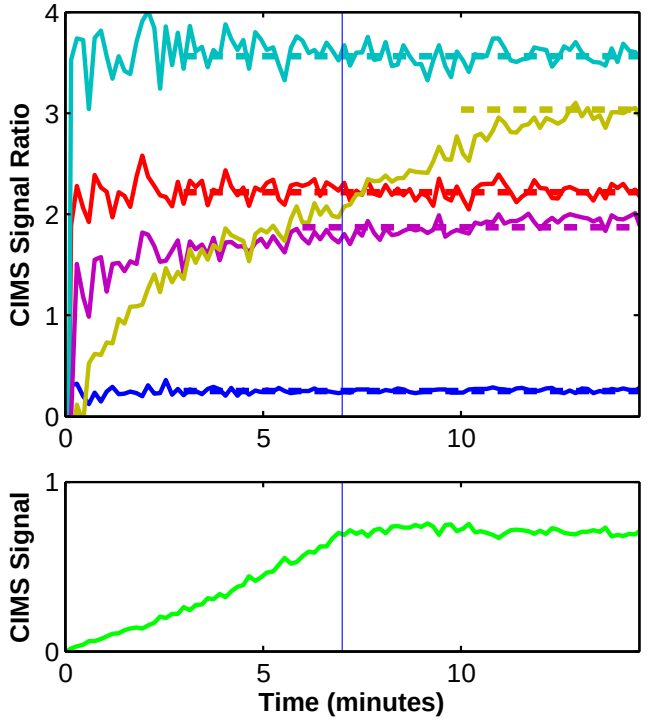

Figure 2. β-hydroxy nitrate products produced from six alkenes during Exp. 19. The top panel shows the ratio of CIMS hydroxy nitrate (HN) signals to propene HN (206 m/z) for ethene HN (192 m/z, blue), methylpropene HN (220 m/z, red), 2-methyl,2-butene HN (234 m/z, teal), 1-hexene HN (248 m/z, purple), and 1-octene HN (276 m/z, gold). The bottom panel shows the absolute signal for propene HN (206 m/z). The lights were turned on at time = 0, and turned off at 7 min (vertical line), at which point the oxidation stopped. For all compounds other than hydroxy nitrates from 1-octene, a ratio is plotted as a dashed line using averaged data from 3 min after lights until the measurements stopped. For hydroxy nitrates from 1-octene, data after 10 min are averaged. The time lag for hydroxy nitrates from 1-octene arises from wall and sample line equilibration. This suggests that the measured yield is a lower limit.

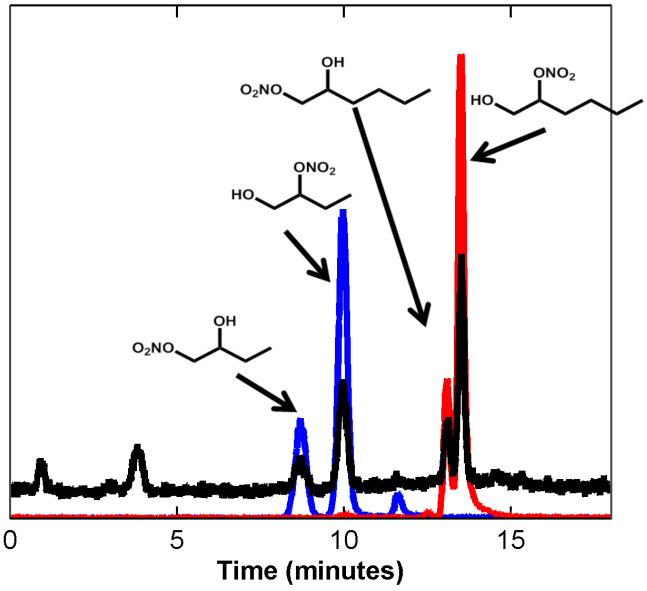

Figure 3. GC-CIMS/TD-LIF chromatogram following Exp. 15. The signals due to individual hydroxy nitrates are determined by integrating the alkyl nitrate peaks (black line, elevated baseline) which co-elute with the individual hydroxy nitrates observed by CIMS, e.g., hydroxy nitrates from 1-butene at 220 m/z (blue) and from 1-hexene at 248 m/z. Absolute CIMS sensitivities are determined by integrating individual peaks for CIMS signal and TD-LIF signal and dividing. The assigned chemical structures are shown for each alkyl nitrate peak.

subscript indicates the carbon at which H-abstraction takes place. Therefore $f_a + f_{ab} = 1$. The isomer-averaged branching ratio (α no subscript) to form β-hydroxy nitrates from OH addition to a mono-alkene is then defined in this paper as $\alpha = f_{an} \times \alpha_{n+1} + f_{an+1} \times \alpha_n$.

Yields of β-hydroxy nitrates ($Y_{\beta HN}$) are defined as the change in hydroxy nitrate concentration over the change in hydrocarbon (HC): $Y_{\beta HN} = -\mathrm{d[HN]/d[HC]}$. Hydroxy nitrates produced via H-abstraction and subsequent alkoxy H-shift isomerization result in molecules with different molecular weights from hydroxy nitrates produced by OH addition, and therefore only β-hydroxy nitrates produced via OH addition are counted in yields. Isomer-averaged branching ratios (α) to form β-hydroxy nitrates from β-hydroxy peroxy radicals can be calculated from β-hydroxy nitrate yields by normalizing for the fraction of the alkene reactions with OH that proceed via OH addition: $\alpha = Y_{\beta HN}/(f_a/(f_a + f_{ab})) = Y_{\beta HN}/f_a$. For alkenes studied here, f_a is greater than 0.75.

3.1 Determination of CIMS sensitivities by TD-LIF for hydroxy nitrates

CIMS sensitivities were derived from cryofocused gas chromatography and simultaneous measurement of β-hydroxy nitrate compounds by CF_3O^- CIMS and TD-LIF. Discrete gaussian peaks which eluted at the same time in the CIMS and TD-LIF were integrated. The time-integrated normalized ion counts from the CIMS was multiplied by the split ratio between TD-LIF and CIMS instruments then divided by the integrated NO_2 signal (ppbv × s) measured by the TD-LIF to determine a sensitivity in normalized counts ppbv of $RONO_2$. Sensitivities are listed in Table 2. An example chromatogram of GC-CIMS/TD-LIF from which sensitivities are derived is shown in Fig. 3.

3.2 The relative yields of β-hydroxy nitrates from alkene oxidation

β-hydroxy nitrate branching ratios were measured relative to $\alpha_{HN\_propene}$ for Experiments 31–36 with the exception of Experiment 31 which measured d_6-propene relative to 1-butene. With minimal oxidation of total hydrocarbon (< 10 %), the

Table 2. Absolute sensitivities for each individual isomer and isomer-averaged sensitivities (bold) were determined by summing peaks in both the CIMS and TD-LIF, and deriving a sensitivity, expressed as normalized counts of analyte ion (normcts) per pptv of analyte. Uncertainties (1σ) include the 10 % uncertainty from the split ratio and absolute NO_2 determination by the TD-LIF. The measured 1-hexene HN sensitivities are lower than other HNs measured in this study. This may reflect precision errors for this one compound, and thus lead to a high biasing in the HN branching of 1-hexene and 1-octene.

Hydroxy nitrates derived from	Measured CIMS CF_3O^- sensitivity (normcts pptv^{-1}), 10^4
ethene, 1-OH, 2-ONO_2	**3.5 ± 0.4**
propene 1-OH, 2-ONO_2	5.0 ± 1.2
propene 2-OH, 1-ONO_2	5.0 ± 1.4
propene, both	**5.0 ± 1.0**
1-butene 1-OH, 2-ONO_2	3.3 ± 0.5
1-butene 2-OH, 1-ONO_2	2.9 ± 0.4
1-butene, both	**3.1 ± 0.4**
cis-2-butene, first diastereomer	2.8 ± 0.4
cis-2-butene, second diastereomer	2.9 ± 0.4
cis-2-butene, both	**2.9 ± 0.4**
methylpropene 1-OH, 2-ONO_2	3.9 ± 0.4
methylpropene 2-OH, 1-ONO_2	3.7 ± 0.8
methylpropene, both	**3.8 ± 0.5**
2-methyl,2-butene 2-OH, 3-ONO_2	3.8 ± 0.4
2-methyl,2-butene 3-OH, 2-ONO_2	3.8 ± 0.5
2-methyl,2-butene, both	**3.8 ± 0.4**
1-hexene, 1-OH, 2-ONO_2	2.6 ± 0.3
1-hexene, 2-OH, 1-ONO_2	2.0 ± 0.4
1-hexene, both	**2.4 ± 0.3**

Absolute sensitivities for all isomers were determined by summing all peaks in both the CIMS and TD-LIF, and deriving a sensitivity from the total. Uncertainties (1σ) include the 10 % uncertainty from the split ratio and absolute NO_2 determination by the TD-LIF. The measured 1-hexene HN sensitivities are lower than other HNs measured in this study. This may reflect precision errors for this one compound, and thus lead to a high biasing in the HN branching of 1-hexene and 1-octene.

measured CIMS signal of each compound is used to determine the ratio of the yield of β-hydroxy nitrates, where yield is defined as $Y = f_{a1} \times \alpha_2 + f_{a2} \times \alpha_1$:

$$\frac{Y_{\mathrm{HN\_alkene}}}{Y_{\mathrm{HN\_propene}}} = \frac{\mathrm{signal}_{\mathrm{HN\_alkene}}}{\mathrm{signal}_{\mathrm{HN\_propene}}} \cdot \frac{\mathrm{sens}_{\mathrm{HN\_propene}}}{\mathrm{sens}_{\mathrm{HN\_alkene}}} \cdot \frac{k_{\mathrm{OH,propene}}}{k_{\mathrm{OH,alkene}}} \cdot \frac{[\mathrm{propene}]_{\mathrm{avg}}}{[\mathrm{alkene}]_{\mathrm{avg}}}. \quad (1)$$

To determine the ratio of the average branching ratios ($\alpha_{\mathrm{alkene}}/\alpha_{\mathrm{propene}}$), we multiply the ratio of the yields by the ratio of the fraction of OH addition (f_a):

$$\frac{\alpha_{\mathrm{HN\_alkene}}}{\alpha_{\mathrm{HN\_propene}}} = \frac{Y_{\mathrm{HN\_alkene}}}{Y_{\mathrm{HN\_propene}}} \cdot \frac{f_{\mathrm{a\_propene}}}{f_{\mathrm{a\_alkene}}}. \quad (2)$$

The mean concentrations throughout the experiment were calculated by averaging the initial and final alkene concentrations. The amount of alkene oxidized could not be accurately determined by GC-FID due to the small fractional change in the mixing ratio. Therefore, the loss was estimated iteratively by using the calculated branching ratio for the hydroxy nitrates (see Sect. 3.3 for derivation of absolute branching ratios used in this calculation). The difference in the determination of $Y_{\beta\mathrm{HN}}$ between using average vs. the initial alkene concentrations was less than 5 % in all cases. CIMS signals from Expt. 19 are shown in Fig. 2. Estimates for secondary loss of hydroxy nitrates by reactions with OH for the relative yield experiments (k_{OH} estimates from Treves and Ruddich, 2003; and Kwok and Atkinson, 1995) using the method described by Atkinson et al. (1982) result in corrections of < 3 % and are neglected in this subset of experiments. For absolute yield determinations, which involved larger OH exposure, the applied corrections are listed in Table 3.

The relative branching ratio data set allows us to directly compare the dependence of α on structure by reducing the uncertainties associated with the measurement and analysis. The analysis of the relative yield experiments also reduces systematic uncertainty through cancellation of correlated errors associated with determination of total chamber volume and the use of the GC-FID. The relative yield determination relies on the ratio of OH rate constants, the ratio of initial alkene concentrations, the ratio of CIMS HN sensitivities, and the ratio of CIMS HN signals. In each relative yield determination, only the ratio of OH rate constants and ratio of HN sensitivities are determined outside the given experiment.

3.3 Normalizing nitrate yields for H-abstraction

To calculate the branching ratio for reaction of RO_2 with NO to form β-hydroxy nitrates following addition of OH and O_2 to alkenes, it is necessary to estimate the fraction of alkene loss, f_a, that proceeds via this channel. A quantitative determination of f_a from our experimental data is not possible because CF_3O^- CIMS is insensitive to singly functionalized carbonyl or nitrate compounds formed from the OH H-abstraction channels. The H-abstraction channel by OH has been measured for propene and *cis*-2-butene to be less than 3 %, and for 1-butene to be 8 ± 3 % (Krasnoperov et al., 2011; Loison et al., 2010, and references therein). There have, however, been few studies of H-abstraction rates for other alkenes at ambient temperatures.

Using theoretical methods, Pfrang et al. (2006a, b) predicted that the chain length should not affect the rate of OH addition to 1-alkenes, and therefore, the increasing abstraction rate with size should scale with additional CH_2 groups. There is, however, disagreement in experimental results about how much the abstraction rate increases with each additional CH_2. Aschmann and Atkinson (2008) measured OH rate constants for a series of 1-alkenes and found that the OH rate constant increases at a rate of 2×10^{-12} cm^3 molec^{-1} s^{-1} per CH_2 group, roughly 25 % higher than for *n*-alkanes (1.4×10^{-12} cm^3 molec^{-1} s^{-1}, determined

Table 3. Absolute hydroxy nitrate (HN) yields from alkenes at 293 K and 993 hPa.

Alkene	Δ Alkene ppbv/%	HN, ppbv	$k^1_{OH,HN}$ ($\times 10^{-11}$) ($cm^3\,molec^{-1}\,s^{-1}$)	k^2_w($\times 10^{-6}$) (s^{-1})	F^3	F^4_{temp}	$Y_{\beta HN}$ (%)	f^5_a	α (%)
ethene	221/21 (±2)	2.6 ± 0.5	0.3	3.8	1.06	1.02	1.3±0.2	1	1.3±0.2
overall ethene									1.3 ± 0.5
propene	38/32 (±3)	1.6 ± 0.4	0.6	1.6	1.05	1.01	4.4±1	0.97	4.6±1
propene	60/37 (±4)	2.4 ± 0.6	0.6	1.6	1.07	1.01	4.3±1	0.97	4.4±1
propene	104/39 (±4)	4 ± 0.8	0.6	1.6	1.07	1.05	4.3±1	0.97	4.5±1
propene	83/31 (±2)	3.7 ± 0.8	0.6	1.6	1.05	1.05	4.7±1	0.97	4.8±1
propene	71/18 (±2)	2.9 ± 0.6	0.6	1.6	1.03	1.04	4.4±1	0.97	4.1±1
propene	68/33 (±2)	2.4 ± 0.5	0.6	1.6	1.09	1.04	4.0±1	0.97	4.1±1
propene	34/21 (±3)	1.2 ± 0.3	0.6	1.6	1.03	1.03	3.7±1	0.97	3.9±1
propene	59/36 (±4)	2.1 ± 0.5	0.6	1.6	1.05	1.06	4.0±1	0.97	4.1±1
propene	42/34 (±4)	1.5 ± 0.4	0.6	1.6	1.05	1.01	3.8±1	0.97	3.9±1
overall propene									4.1 ± 2
1-butene	71/55 (±4)	6.8 ± 1.2	0.7	3.7	1.1	1.06	11±2	0.92	12±2
1-butene	78/43 (±3)	7.6 ± 1.3	0.7	3.7	1.09	1.06	12±2	0.92	13±2
overall 1-butene									12 ± 5
cis-2-butene	85/74 (±5)	8.4 ± 1.3	0.6	4	1.11	1.06	12±2	0.97	12±2
overall *cis*--butene									12 ± 4
methylpropene	166/49 (±3)	13.7 ± 1.9	0.5	6.5	1.05	1.05	9±1	0.97	9±1
overall methylpropene									9 ± 3
2-methyl 1-butene	114/60 (±4)	15.5 ± 3.9	0.8	2	1.08	1.05	15±4	0.95	16±4
overall 2-methyl 1-butene									16 ± 7
2-methyl 2-butene	66/64 (±4)	5.3 ± 0.8	0.8	8.3	1.07	1.04	9±2	0.97	9±2
overall 2-methyl 2-butene									9 ± 4
1-pentene	108/44 (±3)	12 ± 3	0.85	6.7	1.12	1.05	13±3	0.87	15±3
overall 1-pentene									15 ± 6
1-hexene	62/59 (±6)	9.2 ± 1.5	1	10	1.2	1.06	19±3	0.86	22±4
1-hexene	78/43 (±4)	11.8 ± 1.9	1	10	1.13	1.07	18±3	0.86	21±4
1-hexene	91/23 (±2)	14.6 ± 2.4	1	10	1.06	1.06	18±3	0.86	21±4
overall 1-hexene									21 ± 8

[1] Rate constants are from Treves and Ruddich (2003) or estimated based on Treves and Ruddich (2003). [2] All loss rate constants are calculated from post experiment HN signal decay. [3] Correction factor F accounts for loss of hydroxy nitrates due to wall loss and reaction with OH. This factor was calculated using a modified equation for F described by Atkinson et al. (1982), where $k_7 = k_{OH,alkene} \times [OH]_{average}$, and $k_{10} = k_{OH,HN} \times [OH]_{average} + k_w$, where $[OH]_{average}$ is calculated using alkene decay. [4] Correction factor F_{temp} accounts for the change in α in response to temperature variation during the experiment. This factor was estimated using the temperature dependence of α reported by Arey et al. (2001). [5] See text for more details on estimates for normalization for the fraction of OH + alkene that proceeds via OH addition, f_a.

by Kwok and Atkinson, 1995). For this analysis, we assume that f_{ab} is 8 % for 1-butene and, because H-abstraction from non-allylic CH_2 groups is expected to be similar to CH_2 groups in alkanes, we assume that the abstraction rate increases according to the parameterization suggested by Kwok and Atkinson (1995). This implies 15 % H-abstraction for 1-hexene, and 22 % for 1-octene. Using a rate similar to that reported in Aschmann and Atkinson (2008), the abstraction fraction (f_{ab}) for 1-octene would be 28 %.

To estimate abstraction rates for methyl-substituted alkenes, we use an overall k_{OH} of $31.4 \times 10^{-12}\,cm^3\,molec^{-1}\,s^{-1}$ for 1-butene (Atkinson and Arey, 2003), Kwok and Atkinson's (1995) suggested k_{OH} for a CH_3 group of $0.14 \times 10^{-12}\,cm^3\,molec^{-1}\,s^{-1}$, and an 8 % H-abstraction (f_{ab}). We estimate a $k_{OH,abstraction}$ rate constant for a secondary allylic CH_2 group of 2.4×10^{-12}. Using an overall k_{OH} of $26.3 \times 10^{-12}\,cm^3\,molec^{-1}\,s^{-1}$ for propene (Atkinson and Arey, 2003) and an upper limit of 3 % abstraction, we derive an upper limit $k_{OH,abstraction}$ rate constant of a primary allylic CH_3 group of $0.8 \times 10^{-12}\,cm^3\,molec^{-1}\,s^{-1}$. Assuming vinylic hydrogen abstraction rates are negligible, we estimate f_{ab} for *cis*-2-butene, methylpropene, 2-methyl 1-butene, 2-methyl 2-butene to all be less than 5 %.

3.4 Absolute β-hydroxy nitrate yields and branching ratios

The absolute yield of hydroxy nitrates for several of the alkenes was determined in Experiments 1–19. Longer reaction times were necessary to quantify, with sufficient precision, the amount of alkene oxidized. The concentration of hydroxy nitrates at the end of the experiment was determined by measuring the total GC-TD-LIF peak signal which corresponded to a CIMS hydroxy nitrate signal. The initial concentration of alkene was determined by FT-IR and GC-FID, and total loss was determined by the decay in peak area by the GC-FID. In Experiments 11–14, 1,2 butanediol was also added as a reference compound to allow the total loss of

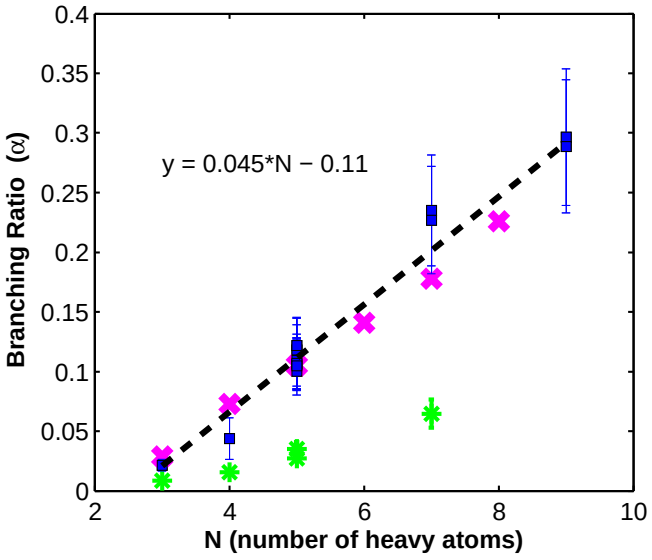

Figure 4. The isomer-averaged branching ratios, α, derived in this study (blue boxes, data from Table 4), compared to previously published nitrate branching ratios (Arey et al., 2001 with pink exes; O'Brien et al., 1998 with green stars). Alkene nitrate yields from O'Brien et al. (1998) have been normalized by f_a to account for H-abstraction channel in the same fashion as this study. The error weighted fit derived from Fig. 4 is shown for hydroxy nitrate branching ratios (black dotted line) from all measured alkenes yields a slope of 0.045 ± 0.016 and intercept of -0.11 ± 0.05 (errors are 2σ). This fit agrees well with the relationship derived by Arey et al. (2001), who calculated a slope of 0.0381 ± 0.0016 and an intercept of -0.073 ± 0.009 for *n*-alkanes.

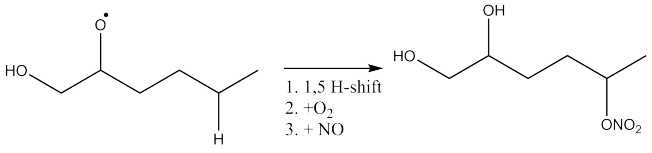

Figure 5. Alkoxy H-shift isomerization leading to dihydroxy nitrate formation for 1-hexene.

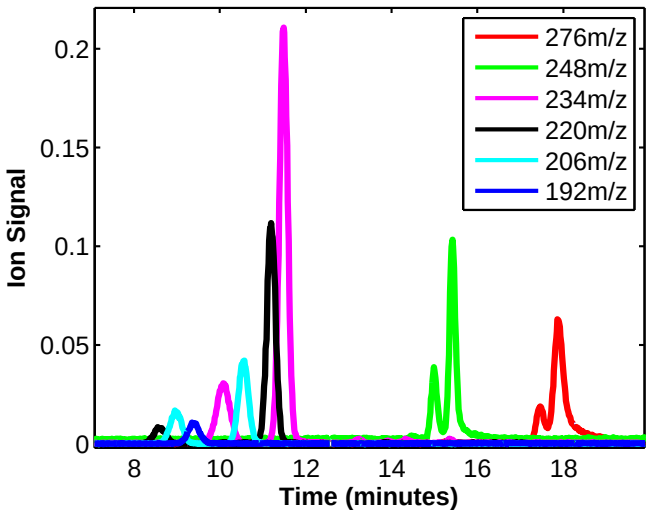

Figure 6. A chromatographic separation of hydroxy nitrates formed from a set of alkenes in Experiment 19. 192 m/z = ethene hydroxy nitrate, 206 m/z = propene hydroxy nitrate; 220 m/z = methylpropene hydroxy nitrate; 234 m/z = 2-methyl 2-butene hydroxy nitrate; 248 m/z = 1-hexene hydroxy nitrate; 276 m/z = 1-octene hydroxy nitrate. Isomer distributions were determined based on integrating peak areas from chromatograms. The later eluting peaks are prone to tailing and co-elution. In such cases, Gaussian peaks shapes were used to deconvolute co-eluting isomers and the trailing tail was assigned to the later eluting peak.

alkene to be determined independent of the GC-FID. 1,2 butane diol was monitored using the CIMS at signal m/z 175 by CIMS to determine its decay over time. The ratio of the OH rate constants for 1,2 butanediol to propene is estimated to be 1.1 ± 0.1 from relative rate information from the literature (Atkinson et al., 1982, 1986; Bethel et al., 2001). The alkene decay inferred from the 1,2 butanediol decay was found to match the GC-FID alkene decay within error. The nitrate yield is calculated by dividing the amount of hydroxy nitrates formed by the amount of alkenes reacted.

For each reaction, a secondary loss correction factor, F, was applied to account for losses of hydroxy nitrates by OH and wall loss using equations derived in Atkinson et al. (1982), and substituting k_7 by $k_7 \times \mathrm{OH}$ and k_{10} by $k_{10} \times \mathrm{OH} + k_w$, where k_w is the experimentally derived first order wall loss rate constant. Rate coefficients for OH + hydroxy nitrates were estimated based on Treves and Ruddich (2003). First order wall loss rate constants were determined by monitoring post-oxidation dark decay over at least an hour and found to be $\leq 10^{-5}\mathrm{s}^{-1}$ for all compounds. A second correction factor, F_{temp}, was applied to normalize the yields to a single temperature ($T = 293$ K) to account for the dependence of the branching ratio on temperature. F_{temp} was estimated using the temperature dependence on branching ratio described in Arey et al. (2001).

Branching ratios to form β-hydroxy nitrates were calculated by normalizing the β-hydroxy nitrate by the fraction of OH + alkene reactions estimated to proceed via OH addition ($\alpha = Y / f_a$). See Sect. 3.4 for more details (Table 3). The yields increase linearly with size of the molecule.

We find that the branching ratios can be expressed as $\alpha = (0.045 \pm 0.016) \times N - (0.11 \pm 0.05)$, where N is the number of heavy atoms in the peroxy radical (not including the peroxy radical oxygens). The α derived for 2-methyl 2-butene was not included in the fit, as it was found to be significantly lower than 1-pentene and 2-methyl 1-butene. Preliminary data from other experiments (not reported here) indicate that α for another internal alkene, 2,3-dimethyl 2-butene, is also substantially lower than similar carbon number compound 1-hexene. It is unclear why these internal alkenes exhibit significantly lower branching ratios to form alkyl nitrates.

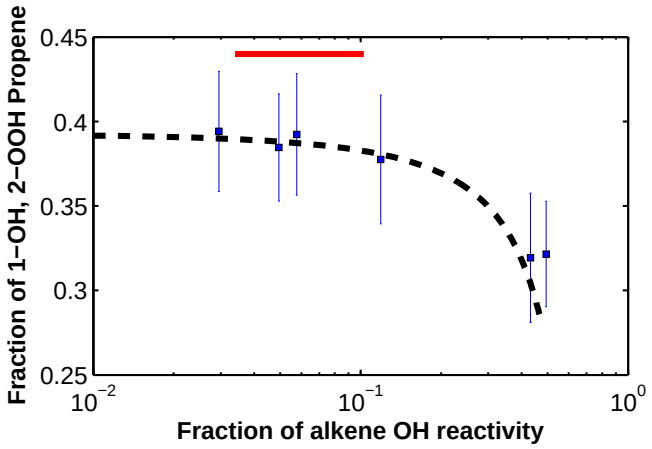

Figure 7. The measured isomer distribution of propene hydroxy hydroperoxides (blue boxes) as a function of the initial alkene OH reactivity and the initial hydrogen peroxide concentration. The red line represents the alkene OH reactivity regime over which hydroxy hydroperoxide isomer distributions were reported for all alkenes other than propene. The dashed black line represents a kinetic box model simulation designed to study the maximum impact $RO_2 + RO_2$ chemistry might have on the isomer distributions. See Appendix B for further details on the kinetic model.

3.5 Hydroxy nitrate branching ratios from relative measurements

To place the relative nitrate yields of the alkenes (3.2) on an absolute basis, we scale the slope of the error weighted fit of the relative branching ratios to match that of the slope of the error weighted fit derived from the observed dependence of the absolute branching ratios on N derived in Sect. 3.3. Branching ratios to form β-hydroxy nitrates calculated using this method are listed in Table 4 and shown in Fig. 4.

The method of placing the relative branching ratios on an absolute basis are prone to correlated errors if the two data sets are not independent of each other. We believe the data sets are sufficiently independent for the following reasons: (1) the absolute nitrate yields require a correction for OH, temperature, and wall loss, whereas the relative set does not, (2) the determination of Δalkene relies on GC-FID for the absolute data set while only initial reactant concentration and literature k_{OH} rate constants for the relative set, (3) the deviations of the data from the best fit relationships are not well correlated. The two data sets, however, are prone to similar biases in the following ways: (1) initial alkene concentrations were measured by FT-IR and with the same reference spectra in both sets of experiments, (2) sensitivities for β-hydroxy nitrates and absolute β-hydroxy nitrate yields both rely upon GC-TD-LIF data.

As shown in Fig. 4, the dependence of the hydroxy nitrate branching ratios from β-hydroxy peroxy radicals on the number of heavy atoms are similar to those observed for peroxy radicals derived from n-alkanes (Arey et al., 2001). This suggests that destabilization of the O–ONO bond due to the presence of the β-hydroxy group is likely small.

Deuteration also leads to an increased branching ratio to form nitrates, possibly due to increased O–ONO lifetime resulting from the lower frequency vibrational and rotational modes. The nitrate branching ratio of d_6-propene is a factor of 1.5 times higher than h_6-propene. A similar increase in nitrate branching ratio has been observed for deuterated isoprene (Crounse et al., 2011).

The measured branching ratios to form β-hydroxy nitrates (Table 4) are consistent with Tuazon et al. (1998) determinations of total alkyl nitrates formed from methylpropene, *cis*-2-butene, and 2-methyl,2-butene. For the experimental conditions in Tuazon et al. (1998), however, formation of methyl nitrate from $CH_3O + NO_2$ may be significant. As the FT-IR nitrate determination includes the sum of all $RONO_2$ species, these results represent an upper limit to the alkene-derived HN yield. Branching ratios reported here are also consistent with those reported by Patchen et al. (2007) for 1-butene and 2-butene determined by CIMS and calibrated using synthesized standards.

The measurements of the branching ratios reported here are significantly higher than those determined by O'Brien et al. (1998) using gas chromatography with calibration using authentic standards. O'Brien et al. (1998) used a similar GC separation technique followed by thermal dissociation of alkyl nitrates with detection of NO_2 by chemiluminescence. The experimental conditions were quite different than the current study. Initial alkene and oxidant concentrations were 2–3 orders of magnitude higher for most alkenes studied. Based on simulations of the experiments reported in O'Brien et al. (1998), the high initial NO concentrations led to rapid production of copious amounts of NO_2, which, upon UV illumination forms significant levels of O^3P for all experiments with initial NO_x concentrations > 100 ppmv. Our simulations suggest that significant alkene loss in their study was due to oxidation by O^3P. This implies a significant underestimation of the branching ratios in the O'Brien et al. (1998) study for all compounds derived from high NO_x experiments. See the Supplement for further details on this analysis.

3.6 Nitrate yields from alkoxy isomerization

In addition to the β-hydroxy nitrates, dihydroxy nitrates are formed from β-hydroxy alkoxy radicals that are able to undergo 1,5 H-shift chemistry (Fig. 5). The CIMS sensitivities for these nitrates could not be obtained because they had low transmission through the gas chromatograph. From ambient sampling, the CIMS signal for the dihydroxy nitrates, relative to the β-hydroxy nitrates, are 1-butene, < 2 %, 1-hexene, > 10 %, 1-octene, > 5 %. For 1-butene, an upper limit is provided due to the small amount formed. For the dihydroxy nitrates from 1-hexene and 1-octene, only lower limits are reported as significant uptake to the walls of the chamber was observed.

Table 4. β HN sensitivities, OH rates, f_a, relative $Y_{\beta HN}$, $\alpha_{alkene}/\alpha_{propene}$ and branching ratios to form β-hydroxy nitrates (HN) at 293 K and 993 hPa.

Alkene	Relative CIMS sensitivity	Relative $k_{OH,alkene}$	Relative $Y_{\beta HN}$	OH addition fraction, f_a[d]	$\alpha_{alkene}/\alpha_{propene}$	α (%)	Previously reported $Y_{total\ N}$ ([a] = only $Y_{\beta HN}$)
ethene	0.7 ± 0.08	0.323 ± 0.04	0.51 ± 0.1	1	0.49 ± 0.1	2.2 ± 0.6	0.86 ± 0.03[a]
ethene	0.7 ± 0.08	0.323 ± 0.04	0.51 ± 0.08	1	0.49 ± 0.08	2.2 ± 0.5	
propene	1 ± 0.2	1 ± 0	1 ± 0.2	0.97	1 ± 0.2	4.4 ± 1	1.5 ± 0.1[a]
d_6-propene	1 ± 0.2[c]	1 ± 0.07	1.5 ± 0.3	1	1.5 ± 0.3	6.6 ± 2	
1-butene	0.62 ± 0.08	1.19 ± 0.05	2.6 ± 0.4	0.92	2.7 ± 0.4	12 ± 3	2.5 ± 0.2[a]
1-butene	0.62 ± 0.08	1.19 ± 0.05	2.6 ± 0.4	0.92	2.8 ± 0.4	12 ± 3	
1-butene	0.62 ± 0.08	1.19 ± 0.05	2.6 ± 0.4	0.92	2.8 ± 0.4	12 ± 3	
cis-2-butene	0.58 ± 0.08	2.13 ± 0.02	2.5 ± 0.4	0.97	2.5 ± 0.4	11 ± 2	3.4 ± 0.5[a]
cis-2-butene	0.58 ± 0.08	2.13 ± 0.02	2.3 ± 0.3	0.97	2.3 ± 0.3	10 ± 2	
methylpropene	0.76 ± 0.1	1.95 ± 0.05	2.4 ± 0.4	0.97	2.4 ± 0.4	10 ± 2	6 ± 2.1[b]
methylpropene	0.76 ± 0.1	1.95 ± 0.05	2.4 ± 0.5	0.97	2.4 ± 0.5	11 ± 3	
methylpropene	0.76 ± 0.1	1.95 ± 0.05	2.4 ± 0.4	0.97	2.4 ± 0.4	11 ± 2	
methylpropene	0.76 ± 0.1	1.95 ± 0.05	2.4 ± 0.4	0.97	2.4 ± 0.4	11 ± 2	
2-methyl 2-butene	0.76 ± 0.08	3.3 ± 0.04	2.5 ± 0.4	0.97	2.5 ± 0.4	11 ± 2	9 ± 3.1[b]
2-methyl 2-butene	0.76 ± 0.08	3.3 ± 0.04	2.4 ± 0.3	0.97	2.4 ± 0.3	10 ± 2	
1-hexene	0.48 ± 0.06	1.4 ± 0.03	4.7 ± 0.8	0.85	5.4 ± 0.9	24 ± 5	5.5 ± 1.0[a]
1-hexene	0.48 ± 0.06	1.4 ± 0.03	4.6 ± 0.7	0.85	5.2 ± 0.8	23 ± 5	
1-octene	0.48 ± 0.06[c]	1.62 ± 0.05	5.5 ± 0.9	0.78	7 ± 1	30 ± 7	13 ± 4.5[b]
1-octene	0.48 ± 0.06[c]	1.62 ± 0.05	4.8 ± 0.7	0.78	6 ± 1	29 ± 6	

[a] O'Brien et al. (1998) only hydroxy nitrate yield; [b] Tuazon et al. (1998); [c] Estimated values. For d_6-propene hydroxy nitrates, the sensitivity is assumed to be the same as propene hydroxy nitrates. For 1-octene hydroxy nitrates, the sensitivity was assumed to be the same as 1-hexene hydroxy nitrates; [d] See the text for how the fraction of reactivity with OH occurring by addition (f_a) is estimated.

3.7 Hydroxy nitrate isomer attribution

An example GC chromatogram is shown in Fig. 6. Transmission through the GC was measured by integrating the entire chromatogram for a given m/z, dividing by direct sampling signal at that same m/z, and multiplying by the ratio of the direct sampling flow rate to the cryofocused gas volume. The transmission for all hydroxy nitrate isomers through the GC-CIMS/TD-LIF was measured to be $100\% \pm 5$ except for 1-octene hydroxy nitrates (transmission $= 92\% \pm 5$).

Peaks were assigned from the GC chromatogram for 1-alkenes assuming the 1-OH addition product is the major isomer due to alkyl radical stabilization (i.e., $f_{a1} > f_{a2}$). In 2-methyl,2-butene, for similar reasons we assume 3-OH addition is formed in higher abundance than 2-OH addition for similar reasons (i.e., $f_{a3} > f_{a2}$). The individual isomeric distributions derived from gas chromatography are listed in Table 5.

3.8 Hydroxy nitrate branching ratios depend on RO_2 substitution

There is significant disagreement in the literature on the dependence of the yield of nitrates from $RO_2 + NO$ with the nature of R. A central question in this debate is whether the yields of nitrates from primary, secondary, and tertiary peroxy radicals are different (Orlando and Tyndall, 2012).

To determine the branching ratios of β-hydroxy alkyl nitrates from specific β-hydroxy peroxy radicals (α_1 and α_2), it is necessary to know the fraction of OH adding to each carbon (f_{a1} and f_{a2}). To estimate these fractions, we measured the isomer distribution of β-hydroxy hydroperoxides formed from the reaction of RO_2 with HO_2. For these peroxy radicals, we assume that the yield of hydroperoxides from $RO_2 + HO_2$ reaction is unity (Raventos-Duran et al., 2007; Hasson et al., 2004; Spittler et al., 2000; Wallington and Japar, 1990a, b). We further assume that the CIMS sensitivity is the same for both isomers. With these assumptions, the ratio of the signal of the hydroxy hydroperoxides to hydroxy nitrate isomers provides an estimate of the difference in nitrate branching ratios for the individual RO_2 isomers.

The hydroxy hydroperoxide isomer distributions are listed in Table 5. It is difficult to ensure that the fate of peroxy radicals (RO_2) react only with HO_2 because the self reaction of HO_2 limits its abundance. There are, therefore, other reaction pathways that must be considered when interpreting the isomer distribution of hydroxy hydroperoxides, namely: $RO_2 + NO$; RO_2 H-shift isomerization, RO_2 + wall, and $RO_2 + RO_2$. $RO_2 + NO$ reactions should not disturb the ROOH isomeric distribution unless the $RO_2 + NO$ reaction rate constant differs between peroxy radicals. We did not detect products resulting from RO_2 H-shift isomerization, nor do we expect for these compounds to undergo H-shift isomerizations given the RO_2 lifetimes (estimated to be < 0.2 s) in these experiments. For similar reasons, RO_2 + wall is not expected to be a large contribution, as the mixing time of our chamber (approximately 5 min) is 2 orders of magnitude slower than the RO_2 lifetime.

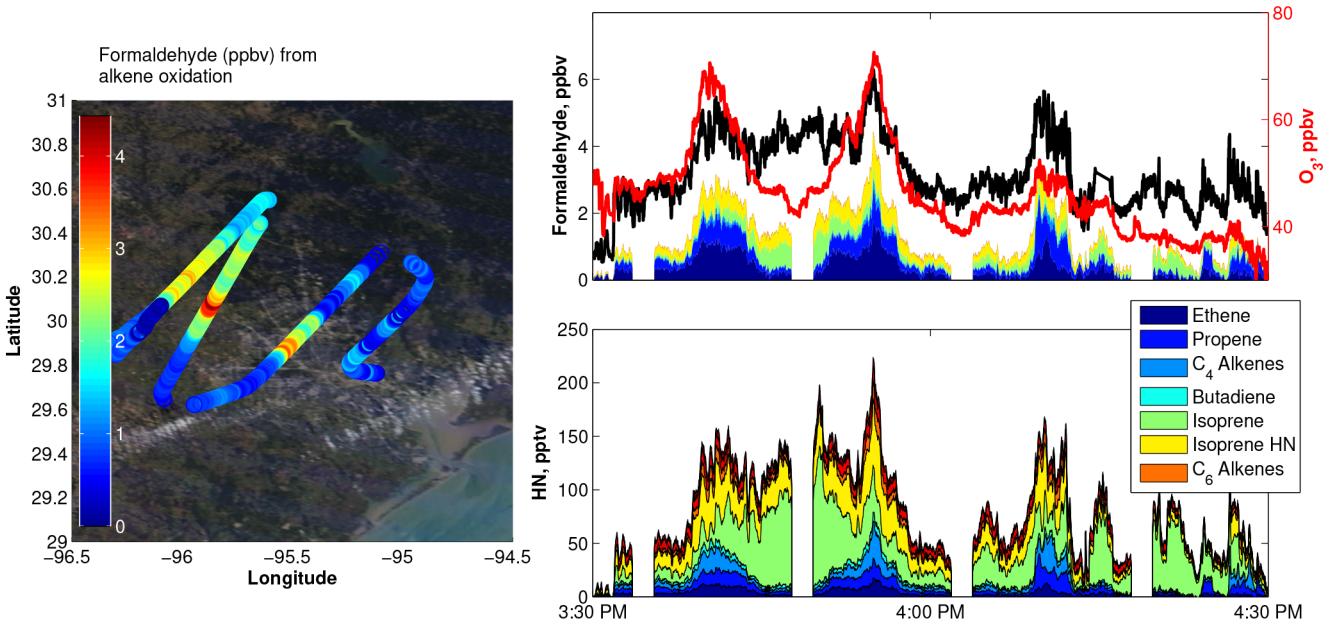

Figure 8. Atmospheric hydroxy nitrate, O_3 and formaldehyde data measured in the Houston plume from the 2013 SEAC4RS campaign. The lower right panel shows how each hydroxy nitrate contributes to the total hydroxy nitrate measured by the Caltech CIMS for the data taken from a flight over Houston on 18 September 2013. As the plane crosses into the Houston plume, hydroxy nitrates derived from anthropogenic emissions are enhanced. The upper right panel shows formaldehyde (black, left axis) and ozone (red, right axis) are strongly correlated with anthropogenically derived hydroxy nitrates. Additionally, the lower bound estimates for the formaldehyde directly attributable to oxidation of each alkene in-plume using the branching ratios derived in this study are shown in colors. For ethene, the contribution is adjusted to produce two formaldehyde molecules after alkoxy decomposition, and uses a decomposition yield of 0.8 to account for glycolaldehyde formation from reaction of the alkoxy radical reaction with O_2. For isoprene hydroxy nitrate, a branching ratio estimate of 0.12 was used (Paulot et al., 2009). It was assumed that the sum of methyl vinyl ketone hydroxy nitrate (MVKN) and methacrolein hydroxy nitrate (MACRN) are exclusively derived from isoprene hydroxy nitrates with a yield of 1 formaldehyde per each isoprene HN oxidized to form a MVKN or MACRN molecule (Lee et al., 2014), and, therefore, a branching ratio estimate of 0.11 was used. Ozone observations were provided courtesy of Ryerson, Pollack and Peischl at NOAA ESRL. Formaldehyde observations provided courtesy of Hanisco and Wolfe at NASA. The left panel graphs the flight tracks for this section of the flight colored by the lower bound estimate of formaldehyde formed from oxidation of alkenes. Satellite image courtesy of NASA's AERONET.

$RO_2 + RO_2$ chemistry will likely perturb the ROOH isomeric distribution due to the strong dependence of peroxy radical self-reaction rates on the alkyl substitution of R (Orlando and Tyndall, 2012, and references therein). We determined the isomer distribution sensitivity to $RO_2 + RO_2$ chemistry with propene by varying the ratio of HO_2 to RO_2 and measuring the subsequent hydroxy hydroperoxide isomer distribution. This was accomplished by increasing the ratio of hydrogen peroxide to initial alkene concentration (and thus the ratio of HO_2 to RO_2) at a given light flux ($j_{H_2O_2} \approx 2 \times 10^{-6} s^{-1}$). Conditions where the propene hydroperoxide isomer ratios reached a plateau were noted, and ratios of the remaining hydroperoxides alkenes were measured at these conditions (see Fig. 7).

The inferred ratio of f_{a1} and f_{a2} is in reasonable agreement with the experimental findings of Cvetanovic (1976) (unpublished, as reported by Peeters et al., 2007), Matsunaga and Ziemann (2009, 2010), Loison et al. (2010), and Peeters et al. (2007) which all found OH addition favors formation of more stable alkyl radicals. In contrast, Krasnoperov et al. (2011) suggested OH addition is equally distributed for propene.

Based on the f_{a1} and f_{a2} and hydroxy nitrate isomer distributions, we find that, for a given compound, the lesser substituted peroxy radical has a lower nitrate branching ratio than the higher substituted peroxy radical. This result is consistent across all compounds studied except 1-hexene, where uncertainty stemming from losses in the GC is large. This finding is in contrast to studies of simple peroxy radicals where α for primary and tertiary radicals have been found to be either equal to or less than α of secondary radicals (Arey et al., 2001; Espada et al., 2005; Cassanelli et al., 2007). Tyndall and Orlando (2012) cautioned that tertiary nitrates may have been underestimated in these studies due to losses of tertiary nitrates in gas chromatography.

A single $RO_2 + HO_2$ experiment (Experiment 37) was conducted with methylpropene to determine whether the assumption of unity yield of hydroxy hydroperoxides was

Table 5. Isomer distribution for hydroxy nitrates and hydroxy hydroperoxides formed from OH addition to alkenes.

Alkene	Product	X = ONO_2 % isomer distribution	X = OOH % isomer distribution	$\alpha_1 : \alpha_2$	Previously reported % distribution	Type of reported distribution
propene	1-X, 2-OH : 2-X, 1-OH	$31 \pm 7 : 69 \pm 7$	$40 \pm 3 : 60 \pm 3$	$1 : 1.5^{+0.3}_{-0.2}$	40 : 60[a]	ONO_2 isomers
					28 : 72[b]	OH branching
					35 : 65[c]	OH branching
					50 : 50[e]	OH branching
					50 : 50[f]	OH branching
1-butene	1-X, 2-OH : 2-X, 1-OH	$27 \pm 7 : 73 \pm 7$	$35 \pm 3 : 65 \pm 3$	$1 : 1.5^{+0.3}_{-0.3}$	44 : 56[a]	$RONO_2$ isomers
					29 : 71[b]	OH branching
					15 : 85[d]	OH branching
cis-2-butene	2-X, 3-OH [(R,S) and (S,R)] : 2-X, 3-OH [(S,S) and (R,R)]	$50 \pm 6 : 50 \pm 6$				
2-methylpropene	1-X, 2-OH : 2-X, 1-OH	$11 \pm 3 : 89 \pm 3$	$21 \pm 2 : 79 \pm 2$	$1 : 2.2^{+0.9}_{-0.6}$	15 : 85[d]	OH branching
2-methyl 2-butene	2-X, 3-OH, 3-methyl : 3-X, 2-OH, 3-methyl	$18 \pm 10 : 82 \pm 10$	$31 \pm 6 : 69 \pm 6$	$1 : 2.0^{+2.4}_{-0.7}$	44 : 66[d]	OH branching
1-hexene	1-X, 2-OH : 2-X, 1-OH	$28 \pm 7 : 72 \pm 7$	$30^{+23}_{-14} : 70^{+14}_{-23}$	$1 : 1.1^{+0.9}_{-0.8}$	42 : 58[a]	$RONO_2$ isomers
1-octene	1-X, 2-OH : 2-X, 1-OH	$14 \pm 15 : 86 \pm 15$				
1-alkene (C_{14} to C_{17})	1-X, 2-OH : 2-X, 1-OH				30 : 70[g]	$RONO_2$ isomers
2-methyl 1-alkene (C_{15})	1-X, 2-OH : 2-X, 1-OH				10 : 90[g]	$RONO_2$ isomers

[a] O'Brien et al. (1998), [b] Loison et al. (2010), [c] Cvetanovic (1976), [d] Peeters et al. (2007), [e] Feltham et al. (2000), [f] Krasnoperov et al. (2011), [g] Matsunaga and Ziemann et al. (2009, 2010).

valid. For methylpropene, the yield of acetone was found to be < 5 % as determined by GC-FID and proton transfer reaction MS. Only an upper bound for acetone production could be estimated due to significant signal interference by hydroxy hydroperoxides to the acetone signal in the GC-FID (see Appendix D).

4 Atmospheric chemistry implications

Measurements of alkyl nitrates in the atmosphere have been used extensively to diagnose ozone and aerosol formation (Rosen et al., 2004; Farmer et al., 2011; Perring et al., 2013). The development of methods described here for speciating these nitrates enables new opportunities to evaluate the role of individual compounds towards oxidant formation in urban regions.

The rate of ozone production from an individual VOC precursor can be estimated from the rate of alkyl nitrate formation. For small molecules where alkoxy chemistry leads to fragmentation, approximately two ozone molecules are formed for each VOC-derived peroxy radical that reacts with NO. In addition, this chemistry yields reactive aldehydes that can lead to further oxidant production.

Neglecting entrainment or deposition and assuming an average alkyl nitrate branching ratio for the VOC mixture $\ll 1$, yields the following relationship (Rosen et al., 2004; Farmer et al., 2011; Perring et al., 2013):

$$\frac{\Delta O_3}{\Delta ANs} \approx \frac{P_{O_3}}{P_{ANs}} \approx \frac{2(1-\alpha)}{\alpha} \approx \frac{2}{\alpha}. \quad (3)$$

In this study, the hydroxy nitrate branching ratios, α, are determined for a suite of alkenes. With this knowledge, we can estimate how much ozone (and, for terminal alkenes, how much formaldehyde) is produced for every alkyl nitrate formed. Recent research flights conducted over Houston as a part of the 2013 NASA SEAC4RS campaign provide an illustration of how measurements of hydroxy nitrates can be used to apportion the role of individual VOC precursors in oxidant formation.

Previous field studies in the Houston–Galveston airshed have yielded contradictory conclusions on the causes for the high ozone episodes experienced in the region. TexAQS I (2000) indicated the direct emission of ethene, propene, butadiene, and butenes were associated with rapid ozone production (Daum et al., 2003; Ryerson et al., 2003; Wert et al., 2003; Zhang et al., 2004). Subsequently, however, data from TexAQS II (2005-6) indicated that primary or secondary emissions of formaldehyde and nitrous acid might contribute significantly to ozone production (Olaguer et al., 2009). Rappengluck et al. (2010) and Buzcu et al. (2011), for example, concluded that a quarter or more of the measured formaldehyde is directly emitted from vehicles. In contrast, Parrish et al. (2012), suggested that greater than 90 % of the formaldehyde is produced via alkene oxidation. The disagreement on the source of formaldehyde has significant implications for ozone mitigation strategies (Olaguer et al., 2014).

Shown in Fig. 8 are Caltech CIMS measurements of hydroxy nitrates above Houston obtained during SEAC4RS flight of 18 September 2013. During this flight, the NASA DC8 aircraft traversed Houston repeatedly sampling plumes of elevated ozone and formaldehyde. The measured hydroxy nitrates are highly correlated with elevated ozone and formaldehyde. Using Eq. (3), we find that the oxidation of small alkenes explains a large fraction of these enhancements. This finding is consistent with the earlier analysis of Rosen et al. (2004), and we suggest that, a decade later, small alkenes from petrochemical emissions remain a significant contributor to oxidant formation in Houston.

5 Conclusion

β-hydroxy nitrate branching ratios for reactions of NO with RO_2 derived from the OH addition to linear and methyl-substituted alkenes are reported. Measurements of the hydroxy hydroperoxide isomer distributions from HO_2-dominated oxidation of propene, 1-butene, 2-methyl 2-butene, methylpropene, and 1-hexene suggest that there is a significant difference in nitrate branching ratio, and that these branching ratios increase with increasing substitution (primary < secondary < tertiary). We recommend the overall β-hydroxy nitrate branching ratio from β-hydroxy peroxy radicals produced from C_2 to C_8 monoalkenes to be $\alpha = (0.045 \pm 0.016) \times N - (0.11 \pm 0.05)$, where N is the total number of heavy atoms (for alkenes, N is the total number of carbon atoms plus 1 for the OH that adds), and listed errors are 2σ. The branching ratio dependence on the number of heavy atoms is found to be the same (within error) to that derived for n-alkanes (Arey et al., 2001).

Appendix A: Uncertainties

The following is a description of the uncertainties associated with each step in the analysis presented here.

1. The determination of CIMS sensitivities for β-hydroxy nitrate compounds.
2. The relative determination of α.
3. The absolute determination of α.
4. The hydroxy nitrate isomer distributions.
5. The hydroxy hydroperoxide isomer distributions.

A1 CIMS sensitivities derived from TD-LIF measurements

The uncertainties associated with determination of the CIMS sensitivity include the following: assumption that the conversion of β-hydroxy nitrates is 100 % in the TD-LIF; uncertainty in the split ratio of eluent flow between the CF_3O^- CIMS and TD-LIF; uncertainty in the absolute sensitivity to NO_2 in the TD-LIF; and integration errors associated with determining a baseline for trailing peaks in both the CF_3O^- CIMS and the TD-LIF chromatograms. Uncertainty in the conversion of hydroxy nitrates in the TD-LIF is discussed in Appendix A. Combined errors for the split flow ratio and absolute NO_2 determination are 10 %. Reproducibility of sensitivity from repeat chromatograms had errors than < 5 %, except for propene (< 15 %), which was signal-to-noise limited. It is possible that co-eluting compounds detectable in the TD-LIF but not the CF_3O^- CIMS would bias the CIMS sensitivity low. For hydroxy nitrates from d_6-propene and 1-octene, the CIMS measurement was assumed to have the same absolute sensitivity as hydroxy nitrates from propene and 1-hexene, respectively. These were estimated to have an additional uncertainty of 3 %.

A2 Relative determination of α

Uncertainty in the estimate of the hydroxy nitrate branching ratios relative to $\alpha_{\text{HN\_propene}}$ from Eq. (2) are determined by the relative uncertainties associated with the direct sampling CIMS measurement, the determination of CIMS sensitivities, the ratio of the OH reaction rate constants from the literature, uncertainties associated with determining the relative initial concentrations and the relative ratio of the secondary loss rates. Relative uncertainties in the k_{OH} rate constants were taken from Atkinson et al. (1983, 1986), and Aschmann and Atkinson (2008), and are reported to be < 6 %. The k_{OH} rate for d_6-propene was taken to be the same as k_{OH} for propene (Stuhl et al., 1998). PNNL spectral database IR cross sections were used to determine alkene gas concentrations, with an associated uncertainty of 2 %. For compounds with no published IR cross sections, the GC-FID signal was used to corroborate the pressure measurement. This contributes an additional 3 % uncertainty. Uncertainties in the CIMS quantification of hydroxy nitrates include background signal subtraction, signal to noise level, and equilibration-related time lags associated with lower volatility compounds. The combination of these uncertainties are estimated to be lower than 10 % for all compounds. Additional uncertainty in sensitivity for d_6-propene and 1-octene hydroxy nitrates was assumed to be 3 % because HNs derived from those compounds were not calibrated using the GC-TD-LIF technique.

A3 Absolute determination of α

As compared to the determination of α relative to $\alpha_{\text{HN\_propene}}$, the absolute determination of α includes significant additional uncertainty associated with determining the total change in alkene concentration, the correction factors, F and F_{temp}, which account for secondary losses of hydroxy nitrates and the effect of increasing temperature from prolonged UV illumination of the chamber. The total change in alkene concentration includes uncertainty from the determination of total chamber volume (3 %) and the GC-FID to quantify alkene loss (tabulated from repeat GC-FID measurements, and listed in Table 2). Secondary losses and temperature effects are tabulated in Table 2, and their uncertainties are taken to be half their total correction value. To determine an overall estimate for the branching ratio for a given compound, a reproducibility uncertainty (20 %, estimated from the standard deviation of the propene experiments) was added to the average of multiple experiments.

A4 β-hydroxy nitrate isomer distributions

Uncertainty estimates include uncertainty propagation from the CIMS sensitivity determination by TD-LIF for individual isomers, reproducibility of peak integration (± 2 % for all compounds), discriminatory losses in the GC for 1-octene, and peak deconvolution for 2-methyl 2-butene HN isomers (an additional 7 %). For all compounds listed, the GC transmission is found to be 100 ± 5 %, except for 1-hexene $RONO_2$, which had a transmission of 92 ± 5 %, which was assigned an additional error from this potentially discriminatory loss.

A5 β-hydroxy hydroperoxide isomer distributions

Uncertainty in the isomer distribution contain contributions from the reproducibility in GC peak integrations, and discriminatory losses through the GC. Uncertainties in the GC peak integrations are < 4 % for all compounds, with an extra uncertainty of < 5 % assigned to 2-methyl 2-butene arising from peak deconvolution of an assumed Gaussian peak shape. For all compounds listed, the GC transmission is found to be 100 ± 5 %, except for 1-hexene derived ROOH, which had a transmission of 50 %. It is unclear for this compound whether the losses through the GC discriminated be-

tween the isomers, and therefore the uncertainties for this isomer distribution are large. Uncertainty from the impact of $RO_2 + RO_2$ was determined to be negligible given that the distribution for propene hydroxy hydroperoxides plateaus at the experimental conditions in this work (Fig. 7). Further evidence for the negligible impact of $RO_2 + RO_2$ is the lack of signals from dihydroxy and hydroxycarbonyl compounds in the CIMS observations. Experiments 25 and 26, conducted at higher ratios of alkene to hydrogen peroxide, had distinct dihydroxy and hydroxy carbonyl signals. The potential impact of $RO_2 + RO_2$ was also estimated through kinetic box modeling in which the primary RO_2 was allowed to react at a fast rate equivalent to peroxyacetyl radicals. The kinetic box modeling results, shown in Fig. 7, suggests that the impact of $RO_2 + RO_2$ on the isomer distribution should be minimal over the experimental conditions. See Appendix C for a full description of the box model used. The uncertainty estimates do not take into account potential differences in the CIMS sensitivity for specific isomers as isomers were assumed to have the same sensitivity. For hydroxy nitrate isomers, aside from the 1-hexene HN, all isomers were determined to have very similar sensitivities.

Appendix B: Conversion efficiency in the TD-LIF

The conversion efficiency of the TD-LIF instrument was evaluated with isopropyl nitrate. A known concentration of isopropyl nitrate was prepared in helium and sampled by the TD-LIF instrument. Oxygen addition upstream of the TD-LIF oven was increased until the NO_2 signal downstream of the oven reached a plateau. This level was equal to the concentration of isopropyl nitrate (Fig. B1).

The conversion of $RONO_2$ in the GC-CIMS/TD-LIF was also evaluated with isopropyl nitrate. A known amount of isopropyl nitrate was added into the chamber filled with air and sampled directly into the TD-LIF, bypassing the GC. A known volume of chamber air was then cryofocused onto the head of the GC column and analyzed in the same way described in Sect. 2. The signal from direct sampling and GC sampling agreed with the gravimetric determination to better than 10 %.

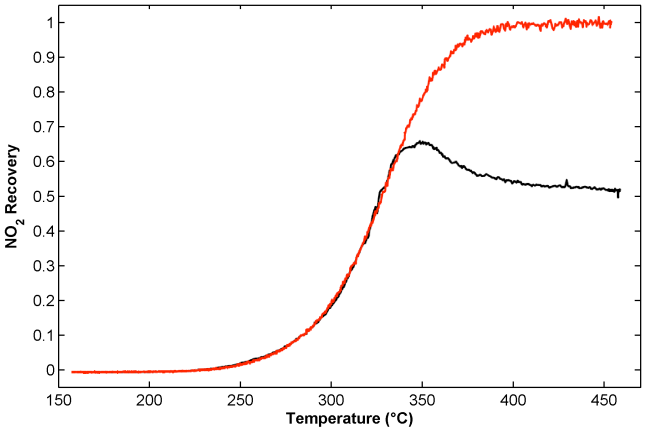

Figure B1. A graph showing the NO_2 recovery as a function of temperature. The NO_2 recovery with addition of O_2 in the TD-LIF is shown in red, and in black is NO_2 recovery without addition of O_2. Conversion of isopropyl nitrate is 100 % in the TD-LIF.

The conversion of the TD-LIF was also evaluated with isoprene hydroxy nitrates (ISOPN). The ISOPN concentrations were measured directly with TD-LIF after addition of only ISOPN into the chamber. This measurement was, however, problematic due to long equilibration times (> 3 h) resulting from low sampling flow and small diameter tubing in the TD-LIF optimized for GC use. The sensitivity as determined by this measurement was 10–30 % greater than the sensitivity determined through the GC for ISOPN compounds. Full equilibration of ISOPN in the direct sampling lines of the TD-LIF was never reached given the limited sampling time available for experiments. Direct sampling of the alkene-derived hydroxy nitrates discussed in this paper was not possible because authentic standards for these compounds were not available, and post-oxidation chamber air contains non-negligible levels of NO_2. Additionally, it has been observed that high concentrations of hydrogen peroxide perturbs the measurements of nitrates and NO_2 in the TD-LIF, particularly in the presence of NO. Using a GC to separate hydrogen peroxide, NO_2 and NO allowed measurements of hydroxy nitrate yields without these interferences.

Table C1. Box modeling reactions

Reactions	Rate constants
$H_2O_2 + h\nu \rightarrow OH + OH$	2×10^{-6}
$H_2O_2 + OH \rightarrow HO_2 + H_2O$	1.8×10^{-12}
$HO_2 + HO_2 \rightarrow H_2O_2$	2.5×10^{-12}
$OH + \text{alkene} \rightarrow 0.4\text{prim}RO_2 + 0.6\text{sec}RO_2$	2.63×10^{-11}
$\text{prim}RO_2 + \text{prim}RO_2 \rightarrow \text{products}$	1.6×10^{-11}
$\text{prim}RO_2 + HO_2 \rightarrow \text{primROOH}$	1×10^{-11}
$\text{sec}RO_2 + HO_2 \rightarrow \text{secROOH}$	1×10^{-11}

All rate constant units are in $cm^3\ molec^{-1}\ s^{-1}$ except for $H_2O_2 + h\nu$, which is in s^{-1}.

Appendix C: Kinetic box modeling for hydroxy hydroperoxide isomer distribution

A kinetic box model of simplified chemistry in the hydroxy hydroperoxide yield experiments was used to understand the maximum potential impact of $RO_2 + RO_2$ reactions on the isomer distribution of hydroxy hydroperoxides. In the simplified chemistry only primary peroxy radicals self reactions are considered to occur with a fast reaction rate constant equivalent to the self reaction of peroxyacetyl radical (Atkinson et al., 2007). A rate constant for the $RO_2 + HO_2$ of 1×10^{-11} $cm^3 molec^{-1} s^{-1}$ (slightly slower than the IUPAC (International Union of Pure and Applied Chemistry) recommended rate constant for hydroxy-ethene $RO_2 + HO_2$; Atkinson et al., 2007) is assumed. The products of $RO_2 + RO_2$ were assumed to be chain terminating to minimize subsequent production of HO_2. The model used the measured ratio of primary to secondary peroxides from propene of 0.39 : 0.61. Table C1 lists the considered reactions and accompanying rate constants. The box model was initialized with 2.5 ppmv H_2O_2 and propene concentrations varying from 1 to 150 ppbv. The box model was run for 10 min, the approximate length of UV exposure for each hydroxy hydroperoxide isomer run.

The model runs suggests that at the ratio of initial alkene OH reactivity to hydrogen peroxide concentration used in this study, the hydroxy hydroperoxide isomer distribution are unaffected by $RO_2 + RO_2$ chemistry.

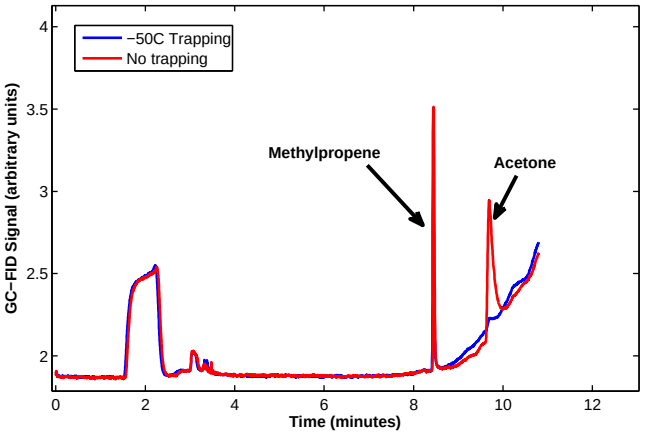

Figure D1. Cold trapping eliminates hydroxy hydroperoxides, removing an interference to the measured acetone.

Appendix D: Measurement of HO_x recycling for methylpropene

Acetone measurements in the GC-FID were used to infer the yield of HO_x recycling for $RO_2 + HO_2$ reactions occurring after OH and O_2 additions to methylpropene. These observations were significantly impacted by methylpropene derived hydroxy hydroperoxides decomposing into acetone in the stainless steel sample loop. Similar decomposition of hydroxy hydroperoxides into carbonyls has been noted in other analytical instrumentation, particularly from isoprene-derived hydroxy hydroperoxides decomposing into methacrolein and methyl vinyl ketone (Liu et al., 2013; Rivera et al., 2014). In order to measure the true acetone signal, a portion of the Teflon sample line was placed in a −50 °C isopropanol bath, a temperature that was sufficiently low to completely trap the hydroxy hydroperoxides while not retaining acetone. Blank GC runs with zero air were run until a negligible acetone signals were measured, at which point cold trapped samples of chamber air were analyzed. The result of removing hydroxy hydroperoxides while retaining acetone is shown in Fig. 2, where the true acetone signal is shown to be low for Experiment 37.

The measurement of acetone was also confirmed with online measurements from the triple quadrupole CIMS instrument operated in positive mode with proton-transfer ionization. The predominant reagent ion in this mode is the protonated double cluster of water, $H_2OH_3O^+$. It was confirmed by measuring methylpropene-derived hydroxy hydroperoxides that this particular sampling and ionization method did not yield ions of protonated acetone from these hydroxy hydroperoxides in any significant yield.

The Supplement related to this article is available online at doi:10.5194/acp-15-4297-2015-supplement.

Acknowledgements. The authors thank T. Ryerson, I. B. Pollack, and J. Peischl at NOAA ESRL for ozone observations and T. F. Hanisco and G. M. Wolfe at NASA for formaldehyde observations from the NASA SEAC4RS flight on 18 September 2013. We acknowledge grant funding from the National Science Foundation (NSF) under grant AGS-1240604 and funding from the National Aeronautics and Space Administration (NASA) under grant NNX12AC06G and NNX14AP46G-ACCDAM.

Edited by: N. M. Donahue

References

Arey, J., Aschmann, S. M., Kwok, E. S. C., and Atkinson, R.: Alkyl nitrate, hydroxyalkyl nitrate, and hydroxycarbonyl formation from the NO_x–air photooxidations of C_5–C_8 *n*-alkanes, J. Phys. Chem. A, 105, 1020–1027, doi:10.1021/jp003292z, 2001.

Aschmann, S. M. and Atkinson, R.: Rate constants for the gas-phase reactions of OH radicals with e-7-tetradecene, 2-methyl-1-tridecene and the C_7–C_{14} 1-alkenes at 295 ± 1 K, Phys. Chem. Chem. Phys., 10, 4159–4164, doi:10.1039/b803527j, 2008.

Aschmann, S. M., Arey, J., and Atkinson, R.: Kinetics and products of the reactions of OH radicals with 4,4-dimethyl-1-pentene and 3,3-dimethylbutanal at 296 ± 2 K, J. Phys. Chem. A, 114, 5810–5816, doi:10.1021/jp101893g, 2010.

Aschmann, S. M., Arey, J., and Atkinson, R.: Formation yields of C_8 1,4-hydroxycarbonyls from OH + *n*-octane in the presence of NO, Environ. Sci. Technol., 46, 13278–13283, doi:10.1021/es3041175, 2012.

Atkinson, R. and Arey, J.: Atmospheric degradation of volatile organic compounds, Chem. Rev., 103, 4605–4638, doi:10.1021/cr0206420, 2003.

Atkinson, R. and Aschmann, S. M.: Rate constants for the reaction of oh radicals with a series of alkenes and dialkenes at 295 ± 1 K, Int. J. Chem. Kinet., 16, 1175–1186, 1984.

Atkinson, R., Aschmann, S. M., Carter, W. P. L., Winer, A. M., and Pitts, J. N.: Alkyl nitrate formation from the nitrogen oxide NO_x–air photooxidations of C_2–C_8 *n*-alkanes, J. Phys. Chem. A, 86, 4563–4569, doi:10.1021/j100220a022, 1982.

Atkinson, R., Tuazon, E. C., and Carter, W. P. L.: Extent of H-atom abstraction from the reaction of the OH radical with 1-butene under atmospheric conditions, Int. J. Chem. Kinet., 17, 725–734, doi:10.1002/kin.550170703, 1985.

Atkinson, R., Tuazon, E. C., and Aschmann, S. M.: Products of the gas-phase reactions of a series of 1-alkenes and 1-methylcyclohexene with the OH radical in the presence of NO, Environ. Sci. Technol., 29, 1674–1680, doi:10.1021/Es00006a035, 1995.

Atkinson, R., Tuazon, E. C., and Aschmann, S. M.: Products of the gas-phase reaction of the OH radical with 3-methyl-1-butene in the presence of NO, Int. J. Chem. Kinet., 30, 577–587, doi:10.1002/(sici)1097-4601(1998)30:8<577::aid-kin7>3.0.co;2-p, 1998.

Barker, J. R., Lohr, L. L., Shroll, R. M., and Reading, S.: Modeling the organic nitrate yields in the reaction of alkyl peroxy radicals with nitric oxide. 2. Reaction simulations, J. Phys. Chem. A, 107, 7434–7444, doi:10.1021/jp034638j, 2003.

Bethel, H. L., Atkinson, R., and Arey, J: Kinetics and products of the reactions of selected diols with the OH radical, Int. J. Chem. Kin., 33, 310–316, doi:10.1002/kin.1025, 2001.

Brown, S. S., deGouw, J. A., Warneke, C., Ryerson, T. B., Dubé, W. P., Atlas, E., Weber, R. J., Peltier, R. E., Neuman, J. A., Roberts, J. M., Swanson, A., Flocke, F., McKeen, S. A., Brioude, J., Sommariva, R., Trainer, M., Fehsenfeld, F. C., and Ravishankara, A. R.: Nocturnal isoprene oxidation over the Northeast United States in summer and its impact on reactive nitrogen partitioning and secondary organic aerosol, Atmos. Chem. Phys., 9, 3027–3042, doi:10.5194/acp-9-3027-2009, 2009.

Buzcu Guven, B. and Olaguer, E. P.: Ambient formaldehyde source attribution in Houston during TexAQS II and TRAMP, Atmos. Environ., 45, 4272–4280, doi:10.1016/j.atmosenv.2011.04.079 2011.

Carter, W. P. L. and Atkinson, R.: Alkyl nitrate formation from the atmospheric photoxidation of alkanes; a revised estimation method, J. Atmos. Chem., 8, 165–173, 1989.

Cassanelli, P., Fox, D. J., and Cox, R. A.: Temperature dependence of pentyl nitrate formation from the reaction of pentyl peroxy radicals with NO, Phys. Chem. Chem. Phys., 9, 4332–4337, doi:10.1039/B700285H, 2007.

Crounse, J. D., McKinney, K. A., Kwan, A. J., and Wennberg, P. O.: Measurement of gas-phase hydroperoxides by chemical ionization mass spectrometry, Anal. Chem., 78, 6726–6732, doi:10.1021/ac0604235, 2006.

Crounse, J. D., Paulot, F., Kjaergaard, H. G., and Wennberg, P. O.: Peroxy radical isomerization in the oxidation of isoprene, Phys. Chem. Chem. Phys., 13, 13607–13613, doi:10.1039/c1cp21330j, 2011.

Crounse, J. D., Knap, H. C., Ornso, K. B., Jorgensen, S., Paulot, F., Kjaergaard, H. G., and Wennberg, P. O.: Atmospheric fate of methacrolein .1. Peroxy radical isomerization following addition of OH and O_2, J. Phys. Chem. A, 116, 5756–5762, doi:10.1021/jp211560u, 2012.

Crounse, J. D., Nielsen, L. B., Jorgensen, S., Kjaergaard, H. G., and Wennberg, P. O.: Autoxidation of organic compounds in the atmosphere, J. Phys. Chem. Lett., 4, 3513–3520, doi:10.1021/Jz4019207, 2013.

Daum, P. H., Kleinman, L. I., Springston, S. R., Nunnermacker, L. J., Lee, Y.-N., Weinstein-Lloyd, J., Zheng, J., and Berkowitz, C. M.: A comparative study of O3 formation in the Houston urban and industrial plumes during the 2000 Texas Air Quality Study, J. Geophys. Res., 108, 4715, doi:10.1029/2003JD003552, 2003.

Espada, C., Grossenbacher, J., Ford, K., Couch, T., and Shepson, P. B.: The production of organic nitrates from various anthropogenic volatile organic compounds, Int. J. Chem. Kinet., 37, 675–685, doi:10.1002/kin.20122, 2005.

Farmer, D. K., Perring, A. E., Wooldridge, P. J., Blake, D. R., Baker, A., Meinardi, S., Huey, L. G., Tanner, D., Vargas, O., and Cohen, R. C.: Impact of organic nitrates on urban ozone produc-

tion, Atmos. Chem. Phys., 11, 4085–4094, doi:10.5194/acp-11-4085-2011, 2011.

Feltham, E. J., Almond, M. J., Marston, G., Wiltshire, K. S., and Goldberg, N.: Reactions of hydroxyl radicals with alkenes in low-temperature matrices, Spectrochim. Acta, 56, 2589–2603, 2000.

Hasson, A. S., Tyndall, G. S., and Orlando, J. J.: A product yield study of the reaction of HO_2 radicals with ethyl peroxy ($C_2H_5O_2$), acetyl peroxy ($CH_3C(O)O_2$), and acetonyl peroxy ($CH_3C(O)CH_2O_2$) radicals, J. Phys. Chem. A, 108, 5979–5989, doi:10.1021/jp048873t, 2004.

Johnson, T. J., Sams, R. L., Blake, T. A., Sharpe, S. W., and Chu, P. M.: Removing aperture-induced artifacts from fourier transform infrared intensity values, Appl. Optics, 41, 2831–2839, 2002.

Krasnoperov, L. N., Butkovskaya, N., and Le Bras, G.: Branching ratios in the hydroxyl reaction with propene, J. Phys. Chem. A, 115, 2498–2508, doi:10.1021/jp107178n, 2011.

Kwok, E. S. C. and Atkinson, R.: Estimation of hydroxyl radical reaction-rate constants for gas-phase organic-compounds using a structure-reactivity relationship – an update, Atmos. Environ., 29, 1685–1695, doi:10.1016/1352-2310(95)00069-B, 1995.

Lee, L., Teng, A. P., Wennberg, P. O., Crounse, J. D., and Cohen, R. C.: On rates and mechanisms of OH and O_3 reactions with isoprene-derived hydroxy nitrates, J. Phys. Chem. A, 118, 1622–1637, doi:10.1021/jp4107603, 2014.

Liu, Y. J., Herdlinger-Blatt, I., McKinney, K. A., and Martin, S. T.: Production of methyl vinyl ketone and methacrolein via the hydroperoxyl pathway of isoprene oxidation, Atmos. Chem. Phys., 13, 5715–5730, doi:10.5194/acp-13-5715-2013, 2013.

Lohr, L. L., Barker, J. R., and Shroll, R. M.: Modeling the organic nitrate yields in the reaction of alkyl peroxy radicals with nitric oxide, 1. Electronic structure calculations and thermochemistry, J. Phys. Chem. A, 107, 7429–7433, doi:10.1021/jp034637r, 2003.

Loison, J. C., Daranlot, J., Bergeat, A., Caralp, F., Mereau, R., and Hickson, K. M.: Gas-phase kinetics of hydroxyl radical reactions with C_3H_6 and C_4H_8: product branching ratios and OH addition site-specificity, J. Phys. Chem. A, 114, 13326–13336, doi:10.1021/jp107217w, 2010.

Matsunaga, A. and Ziemann, P. J.: Yields of beta-hydroxynitrates and dihydroxynitrates in aerosol formed from OH radical-initiated reactions of linear alkenes in the presence of NO_x, J. Phys. Chem. A, 113, 599–606, doi:10.1021/jp807764d, 2009.

Matsunaga, A. and Ziemann, P. J.: Yields of beta-hydroxynitrates, dihydroxynitrates, and trihydroxynitrates formed from OH radical-initiated reactions of 2-methyl-1-alkenes, P. Natl. Acad. Sci. USA, 107, 6664–6669, doi:10.1073/pnas.0910585107, 2010.

Muthuramu, K., Shepson, P. B., and Obrien, J. M.: Preparation, analysis, and atmospheric production of multifunctional organic nitrates, Environ. Sci. Technol., 27, 1117–1124, doi:10.1021/Es00043a010, 1993.

O'Brien, J. M., Czuba, E., Hastie, D. R., Francisco, J. S., and Shepson, P. B.: Determination of the hydroxy nitrate yields from the reaction of C_2–C_6 alkenes with oh in the presence of NO, J. Phys. Chem. A, 102, 8903–8908, doi:10.1021/jp982320z, 1998.

Olaguer, E. P., Rappenglück, B., Lefer, B., Stutz, J., Dibb, J., Griffin, R., Brune, W. H., Shauck, M., Buhr, M., Jeffries, H., Wiuete, W., and Pinto, J. P.: Deciphering the role of radical precursors during the Second Texas Air Quality Study, J Air Waste Manage., 59, 1258–1277, doi:10.3155/1047-3289.59.11.1258, 2009.

Olaguer, E. P., Kolb, C. E., Lefer, B., Rappenglück, B., Zhang R., and Pinto, J. P.: Overview of the SHARP campaign: Motivation, design, and major outcomes, J. Geophys. Res. Atmos., 119, 2597–2610, doi:10.1002/2013JD019730, 2014.

Orlando, J. J. and Tyndall, G. S.: Laboratory studies of organic peroxy radical chemistry: an overview with emphasis on recent issues of atmospheric significance, Chem. Soc. Rev., 41, 6294–6317, doi:10.1039/c2cs35166h, 2012.

Parrish, D. D., Ryerson, T. B., Mellqvist, J., Johansson, J., Fried, A., Richter, D., Walega, J. G., Washenfelder, R. A., de Gouw, J. A., Peischl, J., Aikin, K. C., McKeen, S. A., Frost, G. J., Fehsenfeld, F. C., and Herndon, S. C.: Primary and secondary sources of formaldehyde in urban atmospheres: Houston Texas region, Atmos. Chem. Phys., 12, 3273–3288, /doi10.5194/acp-12-3273-2012, 2012.

Patchen, A. K., Pennino, M. J., Kiep, A. C., and Elrod, M. J.: Direct kinetics study of the product-forming channels of the reaction of isoprene-derived hydroxyperoxy radicals with NO, Int. J. Chem. Kinet., 39, 353–361, doi:10.1002/Kin.20248, 2007.

Paulot, F., Crounse, J. D., Kjaergaard, H. G., Kroll, J. H., Seinfeld, J. H., and Wennberg, P. O.: Isoprene photooxidation: new insights into the production of acids and organic nitrates, Atmos. Chem. Phys., 9, 1479–1501, doi:10.5194/acp-9-1479-2009, 2009.

Peeters, J., Boullart, W., Pultau, V., Vandenberk, S., and Vereecken, L.: Structure-activity relationship for the addition of OH to (poly)alkenes: site-specific and total rate constants, J. Phys. Chem. A, 111, 1618–1631, doi:10.1021/jp066973o, 2007.

Perring, A. E., Pusede, S. E., and Cohen, R. C.: An observational perspective on the atmospheric impacts of alkyl and multifunctional nitrates on ozone and secondary organic aerosol. Chem. Rev., 113, 5848–5870, doi:10.1021/cr300520x, 2013.

Pfrang, C., King, M. D., Canosa-Mas, C. E., and Wayne, R. P.: Structure–activity relations (SARS) for gas-phase reactions of NO_3, OH, and O_3 with alkenes: an update, Atmos. Environ., 40, 1180–1186, doi:10.1016/j.atmosenv.2005.09.080, 2006a.

Pfrang, C., King, M. D., Canosa-Mas, C. E., and Wayne, R. P.: Correlations for gas-phase reactions of NO_3, OH, and O_3 with alkenes: an update, Atmos. Environ., 40, 1170–1179, doi:10.1016/j.atmosenv.2005.10.019, 2006b.

Rappenglück, B., Dasgupta, P. K., Leuchner, M., Li, Q., and Luke, W.: Formaldehyde and its relation to CO, PAN, and SO_2 in the Houston-Galveston airshed, Atmos. Chem. Phys., 10, 2413–2424, doi:10.5194/acp-10-2413-2010, 2010.

Raventos-Duran, T. M., Percival, C. J., McGillen, M. R., Hamer, P. D., and Shallcross, D. E.: Kinetics and branching ratio studies of the reaction of $C_2H_5O_2$ + HO_2 using chemical ionisation mass spectrometry, Phys. Chem. Chem. Phys., 9, 4338–4348, doi:10.1039/b703038j, 2007.

Rivera-Rios, J. C., Nguyen, T. B., Crounse, J. D., Jud, W., St. Clair, J. M., Mikoviny, T., Gilman, J. B., Lerner, B. M., Kaiser, J. B., de Gouw, J., Wisthaler, A., Hansel, A., Wennberg, P. O., Seinfeld, J. H., and Keutsch, F. N.: Conversion of hydroperoxides to carbonyls in field and laboratory instrumentation: Observational bias in diagnosing pristine versus anthropogenically controlled

atmospheric chemistry, J. Geophys. Res. Lett., 41, 23, 1944–8007, doi:10.1002/2014GL061919, 2014.

Rollins, A. W., Browne, E. C., Min, K. E., Pusede, S. E., Wooldridge, P. J., Gentner, D. R., Goldstein, A. H., Liu, S., Day, D. A., Russell, L. M., and Cohen, R. C.: Evidence for NO_x control over nighttime SOA formation, Science, 337, 1210–1212, doi:10.1126/science.1221520, 2012.

Rosen, R. S., Wood, E. C., Thornton, J. A., Day, D. A., Kuster, W., Williams, E. J., Jobson, B. T., and Cohen, R. C.: Observations of total alkyl nitrates during Texas Air Quality Study 2000: implications for O_3 and alkyl nitrate photochemistry, J. Geophys. Res., 109, D07303, doi:10.1029/2003jd004227, 2004.

Ryerson, T. B.: Effect of petrochemical industrial emissions of reactive alkenes and NO_x on tropospheric ozone formation in Houston, Texas, J. Geophys. Res., 108, D084249, doi:10.1029/2002jd003070, 2003.

Sharpe, S. W., Johnson, T. J., Sams, R. L., Chu, P. M., Rhoderick, G. C., and Johnson, P. A.: Gas-phase databases for quantitative infrared spectroscopy, Appl. Spectrosc., 58, 1452–1461, doi:10.1366/0003702042641281, 2004.

Spittler, M., Barnes, I., Becker, K. H., and Wallington, T. J.: Product study of the $C_2H_5O_2 + HO_2$ reaction in 760 torr of air at 284–312 K, Chem. Phys. Lett., 321, 57–61, doi:10.1016/s0009-2614(00)00315-8, 2000.

St Clair, J. M., Rivera-Rios, J. C., Crounse, J. D., Knap, H. C., Bates, K. H., Teng, A. P., Jorgensen, S., Kjaergaard, H. G., Keutsch, F. N., Wennberg, W. O.: Kinetics and products for the reaction of the first generation isoprene hydroxy hydroperoxides (ISOPOOH) with OH, in preparation, 2015.

Stuhl, F.: Determination of rate constants for the reactions of OH with propylene and ethylene by a pulsed photolysis-resonance fluorescence method, Berichte der Bunsengesellschaft für physikalische Chemie, 77, 674–677, 1973.

Treves, K. and Rudich, Y.: The atmospheric fate of C_3–C_6 hydroxyalkyl nitrates, J. Phys. Chem. A, 107, 7809–7817, doi:10.1021/jp035064l, 2003.

Tuazon, E. C., Aschmann, S. M., Arey, J., and Atkinson, R.: Products of the gas-phase reactions of a series of methyl substituted ethenes with the OH radical, Environ. Sci. Technol., 32, 2106–2112, doi:10.1021/Es980153a, 1998.

Tully, F. P. and Goldsmith, J. E. M.: Kinetic-study of the hydroxyl radical propene reaction, Chem. Phys. Lett., 116, 345–352, doi:10.1016/0009-2614(85)80182-2, 1985.

Wallington, T. J. and Japar, S. M.: Reaction of $CH_3O_2 + HO_2$ in air at 295 K – a product study, Chem. Phys. Lett., 167, 513–518, doi:10.1016/0009-2614(90)85461-K, 1990a.

Wallington, T. J. and Japar, S. M.: FTIR product study of the reaction of $CH_3O_2 + HO_2$ in air at 295 K, Chem. Phys. Lett., 166, 495–499, doi:10.1016/0009-2614(90)87140-M, 1990b.

Zhang, D., Zhang, R., Park, J., and North, S. W.: Hydroxy peroxy nitrites and nitrates from OH initiated reactions of isoprene, J. Am. Chem. Soc., 124, 9600–9605, doi:10.1021/ja0255195, 2002.